

hep-ph/9810235
 NT@UW-98-22
 1st October 1998
 Revised 14th April 1999

Power Counting and β Function in NRQCD

Harald W. Griebhammer¹

*Nuclear Theory Group, Department of Physics, University of Washington,
 Box 351 560, Seattle, WA 98195-1560, USA*

Abstract

A computation of the NRQCD β function both in the Lorentz gauge family and in the Coulomb gauge to one loop order endorses a velocity power counting scheme for dimensionally regularised NRQCD. In addition to the ultrasoft scale represented by bremsstrahlung gluons and the potential scale with Coulomb gluons and on-shell quarks, a soft régime is identified in which energies and momenta are of order Mv , gluons are on shell and the quark propagator becomes static. The instantaneous gluon propagator has a non-zero vacuum polarisation only because of contributions from this régime, irrespective of the gauge chosen. Rules are derived which allow one to read up from a given graph whether it is zero because of the homogeneity of dimensional regularisation. They also apply to threshold expansion and are used to prove that ultrasoft quarks with energy and momentum of order Mv^2 decouple from the theory.

Suggested PACS numbers: 12.38.Bx, 12.39.Hg, 12.39.Jh, 11.10.Gh.

Suggested Keywords: Non-Relativistic QCD, Heavy Quark Effective Theory, effective field theory, threshold expansion, renormalisation, β function, dimensional regularisation.

¹Email: hgrie@phys.washington.edu

1 Introduction

Non-Relativistic QCD [1, 2] takes advantage of the fact that when a heavy quark is nearly on shell and its energy is dominated by its mass M , the resulting non-relativistic system exhibits two small expansion parameters: the coupling constant g and the particle velocity v . The Coulomb interaction rules the level spacing in Charmonium and Bottomium because α_s is small enough for perturbative calculations and the relative velocity of the quarks is $v \sim \alpha_s(Mv)$ by virtue of the virial theorem, where the scale of g is set by the inverse Bohr radius Mv of the system. Albeit α_s increases with decreasing $Q^2 \sim (Mv)^2$, a window between the relativistic perturbative and the confinement régime remains in which both α_s and v is small (e.g. for Bottomium, $\alpha_s(M_b v) \approx 0.35$). Therefore, wave functions and potentials obtained by re-summation of ladder diagrams involving relevant couplings as $v \rightarrow 0$ may be used to account for bound state physics, and calculations of production cross sections, hyperfine splittings, lifetimes, threshold properties etc. are much facilitated. The Abelian analogue, NRQED, to which all considerations in this article apply equally well, has also simplified precision calculations in Positronium. An incomplete list of recent references may include [3]–[12].

The NRQCD Lagrangean in terms of the heavy quark (anti-quark) bi-spinors Q (\bar{Q}) and gluons ($D_\mu = \partial_\mu + igA_\mu$) reads

$$\begin{aligned} \mathcal{L}_{\text{NRQCD}} = & Q^\dagger (i\partial_0 - gA_0) Q + \frac{c_1}{2M} Q^\dagger \vec{D}^2 Q + \frac{c_2}{8M^3} Q^\dagger \vec{D}^4 Q + \dots \\ & + \frac{gc_3}{2M} Q^\dagger \vec{\sigma} \cdot \vec{B} Q + \dots - \frac{g^2 d_1}{4M^2} (C\bar{Q}^\dagger \vec{\sigma} Q) \cdot (Q^\dagger \vec{\sigma} C\bar{Q}) + \dots \\ & - \frac{e_1}{4} F_{\mu\nu}^a F^{\mu\nu, a} + \frac{g^3 e_2}{480\pi^2 M^2} F_{\mu\nu}^a D^2 F^{\mu\nu, a} + \dots + \mathcal{L}_{\text{GFix}} , \end{aligned} \quad (1.1)$$

where the coefficients c_i, d_i, e_i, \dots encode the ultraviolet physics: All excitations with four-momenta of the order of M and higher are integrated out and give rise e.g. to four-point interactions between quarks ($d_1 \neq 0$). The perturbative part of the coefficients can be determined by matching NRQCD matrix elements to their QCD counterparts in the régime where both theories are perturbative in the coupling constant. This has been performed to $\mathcal{O}(M^{-3})$ [13]. At tree level, a Foldy-Wouthuysen transformation gives $c_i = 1, e_1 = 1$, and loop corrections are down by powers of g , the most famous example being the coefficient for the Fermi term related to the anomalous magnetic moment of the electron, $c_3 = 1 + \frac{\alpha_s}{2\pi} + \dots$. Further coefficients to enter at one loop level are $d_1 = e_2 = 1$. Lorentz invariance demands $c_1 = c_2 = 1$ to all orders.

The Lagrangean (1.1) consists of infinitely many terms constrained only by the symmetries of the theory and is non-renormalisable. Predictive power is nonetheless established when only a finite number of terms contribute to a given order in the two expansion parameters¹, g and v . Besides the heavy quark mass M , the typical binding energy and momentum scales in NRQCD are the non-relativistic kinetic energy Mv^2 and the momentum Mv of the quark, which in Quarkonia appear as the energy and inverse size of

¹For clarity, the two will be distinguished in the following, although $v \sim \alpha_s$, as noted above.

the bound state [1, 2]. Since for the smallest of the three scales $\alpha_s(Mv^2) \not\ll 1$ in Bottomium and Charmonium, an expansion in g is justified only for the interactions taking place on scales Mv and higher in the real world, but one can imagine a world in which $Mv^2 \gg \Lambda_{\text{QCD}}$. Toponium fulfils this requirement but decays mainly weakly and very fast so that QCD effects do not dominate.

Because the effective Lagrangean does not exhibit the non-relativistic expansion parameter v explicitly, a power counting scheme has to be established which determines uniquely which terms in the Lagrangean must be taken into account to render consistent calculations and predictive power to a given accuracy in v . It is at this point that NRQCD can serve as a “toy model” for nuclear physics [14] (although this grossly understates its value²): It will establish what the relevant kinematic régimes and infrared variables are in a theory with three (or more) separate scales, and it will demonstrate how to count powers of the non-relativistic expansion parameter, v . Recently, velocity power counting rules were established for a toy model [15] following Beneke and Smirnov’s threshold expansion [16], which has become very useful for understanding non-relativistic effective theories. The relevant energy and momentum régimes and low energy degrees of freedom were found for dimensionally regularised non-relativistic theories. This article presents the extension to NRQCD and as an application the calculation of the NRQCD β function. It will also be argued that the diagrammatic approach advocated here sheds a new light on threshold expansion [16] and helps simplify calculations.

Both from a conceptual and a technical point of view the calculation of the NRQCD β function proves interesting. NRQCD is a well-defined field theory of quarks and gluons. One can therefore investigate its renormalisation group equations under the assumption that perturbation theory is applicable at all scales. For example, the running and mixing of the dimension six operators has been investigated to one loop order by Bauer and Manohar [17]. On the other hand, as NRQCD is the low energy limit of QCD, it must reproduce the QCD β function with N_F light quarks below the scale M , but this has not been demonstrated so far. The problem with the power counting developed until now [14, 18, 19] was that gluons mediating the Coulomb interaction (“potential gluons”) seemed to have a vanishing vacuum polarisation and hence a β function which was neither gauge invariant nor agreed with the QCD result, while the coupling of gluons on a much lower scale which mediate bremsstrahlung processes ran as expected. The apparent impasse which results is resolved in this article.

Straightforward as the computation may thus seem with its outcome already anticipated, the prime goal of this article is not the result for the NRQCD β function; the objective is rather to shed more light on power counting in NRQCD and to provide a comparison between calculations in the effective and the full theory. It will show that the Lorentz gauge family (and indeed any standard gauge) is a legitimate gauge choice in NRQCD, not only the Coulomb gauge. It will prove that the recently discussed soft régime [15, 16, 20] with quarks and gluons of four-momenta of order Mv is indispensable for NRQCD to describe the correct infrared limit of QCD. It will also test the validity

²The most striking difference to nuclear physics is that NRQCD has no exceptionally large scattering length to accommodate.

of the power counting proposed. In the Coulomb gauge, it will demonstrate that the renormalisation of the quark propagator and of the leading order quark gluon vertex are trivial, so that for the β function in this gauge, only a computation of the gluon vacuum polarisation is necessary. From a technical point of view, dimensional regularisation for non-covariant loop integrals proves to be a simple regulator choice. It allows to develop a set of simple diagrammatic rules to determine which graphs yield non-zero contributions in perturbation theory. This reduces the computational effort considerably as compared to other regularisation schemes in which power divergences are present like e.g. when using a lattice cut-off. Because of the association of threshold expansion and NRQCD, such rules can be applied to the former, too. Finally, the calculation of the NRQCD β function presented here is – especially in the Feynman gauge – simpler than its QCD counterpart and shows some pedagogically intriguing aspects.

The article is organised as follows: In Sect. 2, the velocity power counting of NRQCD is presented. The relevant régimes of NRQCD are identified (Sect. 2.1), extending the formalism of Luke and Savage [18] by the soft régime of Beneke and Smirnov [16]. The section then proposes the rescaling rules necessary for a Lagrangean with manifest velocity power counting (Sect. 2.2) and gives the vertex (Sect. 2.3) and loop velocity power counting rules (Sect. 2.4). Gauge invariance of the power counting is addressed in Sect. 2.5. The calculation of the NRQCD β function in the Lorentz gauges in Sect. 3 starts by highlighting the intimate relation between threshold expansion and the proposed NRQCD power counting, which will additionally be summarised in the Conclusions. Diagrammatic rules developed in Sect. 3.2 help to facilitate the calculation considerably and are used in Sect. 3.3 to prove the absence of ultrasoft heavy quarks. As a tilly, the β function is computed in the Coulomb gauge in Sect. 3.7. Summary and outlook conclude the article, together with an appendix containing exemplary calculations in non-covariant dimensional regularisation.

2 Velocity Power Counting

2.1 Régimes of NRQCD

The first power counting rules for NRQCD were derived by Lepage et al. [21] in the Coulomb gauge using the consistency of the equations of motion and a momentum cut-off. Only Coulomb gluons with typical momenta of order Mv were considered, taking into account retardation, but neglecting bremsstrahlung effects. The power counting also held to all orders only after all power divergences were subtracted.

Simpler counting rules were proposed by Luke and Manohar for Coulomb interactions [14], and by Grinstein and Rothstein for bremsstrahlung processes [19]. Luke and Savage [18] united these schemes using dimensional regularisation, so that the tree level power counting is automatically preserved to all orders in perturbation theory up to logarithmic corrections. They also extended the formalism to include the Lorentz gauges. Labelle [22] proposed a similar scheme in time ordered perturbation theory. Beneke and

Smirnov [16] observed that the collinear divergence of the two gluon exchange contribution to Coulomb scattering between non-relativistic particles near threshold is not reproduced in this version of NRQCD because the soft low energy régime is not taken into account. A recent article [15] has shown that an extension of the work in [14, 18, 19] using dimensional regularisation, as motivated from threshold expansion [16], resolves this conflict in a toy model. The complete power counting scheme of NRQCD is presented briefly in the following (see also [20]). In Sect. 3.1, the intimate relation between NRQCD as developed in recent years [14, 15, 18, 19] and threshold expansion is addressed in more detail.

The NRQCD propagators are read up from the Lagrangean (1.1) as

$$Q : \frac{i \text{ Num}}{T - \frac{\vec{p}^2}{2M} + i\epsilon} , \quad A^\mu : \frac{i \text{ Num}}{k^2 + i\epsilon} , \quad (2.1)$$

where $T = p_0 - M = \frac{\vec{p}^2}{2M} + \dots$ is the kinetic energy of the quark. “Num” are numerators containing the appropriate colour, Dirac and flavour indices, all of which are unimportant for the considerations in this section and will be suppressed throughout this article. Gauge dependence of the gluon propagator for the power counting is addressed in Sect. 2.5.

Cuts and poles in scattering amplitudes close to threshold stem from saddle points of the loop integrand, corresponding to bound states and on-shell propagation of particles in intermediate states. They give rise to infrared divergences and in general dominate contributions to scattering amplitudes. With the two low energy scales at hand, and energies and momenta being of either scale, three régimes are identified in which either the quark or the gluon in (2.1) is on shell, as noted by Beneke and Smirnov [16]:

$$\begin{aligned} \text{soft régime:} \quad & A_s^\mu : \quad k_0 \sim |\vec{k}| \sim Mv , \\ \text{potential régime:} \quad & Q_p : \quad T \sim Mv^2 , \quad |\vec{p}| \sim Mv , \\ \text{ultrasoft régime:} \quad & A_u^\mu : \quad k_0 \sim |\vec{k}| \sim Mv^2 \end{aligned} \quad (2.2)$$

Note that the scale M has been integrated out when deriving the non-relativistic Lagrangean (1.1), so that a “hard” régime with on shell gluons and quarks of four-momentum of order M cannot be considered.

What is the particle content of each of the three régimes? Ultrasoft gluons A_u^μ are emitted as bremsstrahlung or from excited states in the bound system, and hence are physical. Soft gluons A_s^μ do not describe bremsstrahlung: Because in- and outgoing quarks Q_p are close to their mass shell, they have an energy of order Mv^2 . Therefore, overall energy conservation forbids all processes with outgoing soft gluons but without ingoing ones, and vice versa, as their energy is of order Mv . Finally, gluons which change the quark momenta but keep them close to their mass shell relate the (instantaneous) Coulomb interaction:

$$A_p^\mu : \quad k_0 \sim Mv^2 , \quad |\vec{k}| \sim Mv \quad (2.3)$$

When a soft gluon A_s^μ couples to a potential quark Q_p , the outgoing quark is far off its mass shell and carries energy and momentum of order Mv . Therefore, consistency requires the existence of quarks in the soft régime as well,

$$Q_s : \quad T \sim |\vec{p}| \sim Mv . \quad (2.4)$$

With these five fields $Q_s, Q_p, A_s^\mu, A_p^\mu, A_u^\mu$ representing quarks and gluons in the three different non-relativistic régimes, soft, potential and ultrasoft, NRQCD becomes self-consistent. These fields are the infrared-relevant degrees of freedom representing one and the same non-relativistic particle in the respective kinematic régimes and came naturally by identifying all possible particle poles in the non-relativistic propagators. Their interactions are fixed by the non-relativistic Lagrangean (1.1). Section 3.3 will prove that a hypothetical ultrasoft quark, created e.g. by the radiation of a potential gluon off a potential quark, decouples completely from the theory. On the other hand, Sect. 3 will demonstrate that in order to obtain the correct result for the NRQCD β function, all fields listed above in the three régimes have to be accounted for. Therefore, the particle content presented above is not only consistent but both minimal and complete.

In order to guarantee that there is no overlap between interactions and particles in different régimes, the regularisation scheme must finally be chosen such that the expansion around one saddle point in the loop integral as performed above does not obtain any contribution from other régimes, represented by other saddle points in the loop integrals. One might use an energy and momentum cut-off separating the soft from the potential, and the potential from the ultrasoft régime, but the integrals encountered can in general not be performed analytically and in closed form. Furthermore, by introducing another, artificial scale, cut-off regularisation jeopardises power counting and symmetries (gauge, chiral, ...). Power divergences occur when the (un-physical) cut-off is removed in intermediate steps but not in the final, physical result, complicating the computation. In contradistinction, using dimensional regularisation *after* the saddle point expansion preserves power counting because its homogeneity guarantees that contributions from different saddle points and régimes do not overlap. (A simple example is given in Ref. [15].) Homogeneity will also be essential when developing diagrammatic rules to classify graphs as zero in Sect. 3.2 and when showing the decoupling of the ultrasoft quark in Sect. 3.3.

2.2 Rescaling Rules and Propagators

In order to establish explicit velocity power counting in the NRQCD Lagrangean, one rescales the space-time coordinates such that typical momenta in either régime are dimensionless, as proposed by Luke and Manohar [14] for the potential régime and by Grinstein and Rothstein [19] for the ultrasoft one:

$$\begin{aligned} \text{soft:} \quad & t = (Mv)^{-1} T_s \quad , \quad \vec{x} = (Mv)^{-1} \vec{X}_s \quad , \\ \text{potential:} \quad & t = (Mv^2)^{-1} T_u \quad , \quad \vec{x} = (Mv)^{-1} \vec{X}_s \quad , \\ \text{ultrasoft:} \quad & t = (Mv^2)^{-1} T_u \quad , \quad \vec{x} = (Mv^2)^{-1} \vec{X}_u \quad . \end{aligned} \tag{2.5}$$

For the propagator terms in the NRQCD Lagrangean to be normalised as order v^0 , one sets for the representatives of the gluons in the three régimes [15, 20]

$$\begin{aligned} \text{soft:} \quad & A_s^\mu(\vec{x}, t) = (Mv) \mathcal{A}_s^\mu(\vec{X}_s, T_s) \quad , \\ \text{potential:} \quad & A_p^\mu(\vec{x}, t) = (Mv^{\frac{3}{2}}) \mathcal{A}_p^\mu(\vec{X}_s, T_u) \quad , \\ \text{ultrasoft:} \quad & A_u^\mu(\vec{x}, t) = (Mv^2) \mathcal{A}_u^\mu(\vec{X}_u, T_u) \quad , \end{aligned} \tag{2.6}$$

$$\begin{aligned} \text{soft:} \quad & Q_s(\vec{x}, t) = (Mv)^{\frac{3}{2}} Q_s(\vec{X}_s, T_s) \quad , \\ \text{potential:} \quad & Q_p(\vec{x}, t) = (Mv)^{\frac{3}{2}} Q_p(\vec{X}_s, T_u) \quad . \end{aligned} \tag{2.7}$$

$$\text{soft:} \quad Q_s(\vec{x}, t) = (Mv)^{\frac{3}{2}} \mathcal{Q}_s(\vec{X}_s, T_s) \quad , \quad (2.7)$$

potential: $Q_p(\vec{x}, t) = (Mv)^{\frac{3}{2}} Q_p(\vec{X}_s, T_u) \quad .$

The rescaled free quark Lagrangean reads then

$$\text{soft:} \quad d^3X_s \, dT_s \, \mathcal{Q}_s^\dagger \left(i\partial_0 + \frac{v}{2} \vec{\partial}^2 \right) \mathcal{Q}_s \quad , \quad (2.8)$$

$$\text{potential:} \quad d^3 X_s \, dT_u \, \mathcal{Q}_p^\dagger \left(i \partial_0 + \frac{1}{2} \vec{\partial}^2 \right) \mathcal{Q}_p \quad . \quad (2.9)$$

Here, as in the following, the positions of the fields have been left out whenever they coincide with the rescaled variables of the volume element. Derivatives are to be taken with respect to the rescaled variables of the volume element unless otherwise stated. In order to maintain velocity power counting, corrections of order v or higher must be treated as insertions, so that one reads up the (un-rescaled) quark propagators and insertion as

$$\text{soft:} \quad Q_s : \text{ } \overline{\hspace{0.5cm}} \overline{\hspace{0.5cm}} \text{ } \xrightarrow{(T, \vec{p})} \text{ } \overline{\hspace{0.5cm}} \overline{\hspace{0.5cm}} \text{ } : \frac{i}{T + i\epsilon} \text{ , } \overline{\hspace{0.5cm}} \overline{\hspace{0.5cm}} \text{ } \xrightarrow{(T, \vec{p})} \overline{\hspace{0.5cm}} \overline{\hspace{0.5cm}} \text{ } : -i \frac{\vec{p}^2}{2M} = \text{P.C.}(v^1) \text{ , } (2.10)$$

$$\text{potential: } Q_p : \overset{(T, \vec{p})}{\longrightarrow} : \frac{i}{T - \frac{\vec{p}^2}{2M} + i\epsilon} . \quad (2.11)$$

The soft quark becomes static because $T \sim Mv \gg \frac{\vec{p}^2}{2M} \sim Mv^2$ allows one to expand the non-relativistic propagator (2.1) and to treat the momentum term as an insertion.

Throughout this article, the symbol $\text{P.C.}(v^n)$ denotes at which order in the velocity power counting a certain term or diagram contributes. In the approach presented, each line in a loop diagram counts as $\text{P.C.}(v^0)$ because the strength of the propagator has been set to unity in the rescaled Lagrangean (2.8/2.9). The rescaled Lagrangean measures the strength of the insertion relative to the propagator. Therefore, the soft quark insertion (2.10) does not count as $\frac{\vec{p}^2}{2M}$ which scales like v^2 , but as $\frac{\vec{p}^2}{2M}/T = \text{P.C.}(v)$. In contradistinction to the approach in [16], one will therefore not obtain the absolute order in v at which a given graph contributes, but the relative order in v between graphs or vertices is read off more easily and asserted correctly.

The gauge fixing term was included in the NRQCD Lagrangean (1.1) since the decomposition of the Lagrangean into a free and an interacting part is gauge dependent. Because of the difference between canonical and physical momentum, it is important to specify the gauge *before* identifying to which order in v a certain régime in the Lagrangean contributes, as will be seen shortly. In the following, the Feynman rules for the Lorentz gauges and for the Coulomb gauge are derived explicitly. Sect. 2.5 will comment on the gauge invariance of the procedure.

The rescaled free gluon Lagrangean in the Lorentz gauges reads

$$\text{soft:} \quad d^3X_s \, dT_s \, \frac{1}{2} \, \mathcal{A}_s^\mu \left[\partial^2 g_{\mu\nu} - \left(1 - \frac{1}{\alpha}\right) \partial_\mu \partial_\nu \right] \mathcal{A}_s^\nu \quad , \quad (2.12)$$

$$\begin{aligned} \text{potential:} \quad d^3X_s dT_u \frac{1}{2} \mathcal{A}_p^\mu & \left[g_{\mu\nu} (v^2 \partial_0^2 - \vec{\partial}^2) - \right. \\ & \left. - (1 - \frac{1}{\alpha}) (v \delta_{\mu 0} \partial_0 + \delta_{\mu i} \partial_i) (v \delta_{\nu 0} \partial_0 + \delta_{\nu i} \partial_i) \right] \mathcal{A}_u^\nu, \end{aligned} \quad (2.13)$$

$$\text{ultrasoft:} \quad d^3X_u dT_u \frac{1}{2} \mathcal{A}_u^\mu \left[\partial^2 g_{\mu\nu} - (1 - \frac{1}{\alpha}) \partial_\mu \partial_\nu \right] \mathcal{A}_u^\nu, \quad (2.14)$$

while in the Coulomb gauge

$$\text{soft:} \quad d^3X_s dT_s \frac{1}{2} \mathcal{A}_{i,s} \left[(\vec{\partial}^2 - \partial_0^2) \delta_{ij} - \partial_i \partial_j \right] \mathcal{A}_{j,s}, \quad (2.15)$$

$$\text{potential:} \quad d^3X_s dT_u \frac{1}{2} \left[\mathcal{A}_{0,p} \vec{\partial}^2 \mathcal{A}_{0,p} + \mathcal{A}_{i,p} (\vec{\partial}^2 \delta_{ij} - \partial_i \partial_j - v^2 \partial_0^2 \delta_{ij}) \mathcal{A}_{j,p} \right], \quad (2.16)$$

$$\text{ultrasoft:} \quad d^3X_s dT_s \frac{1}{2} \mathcal{A}_{i,u} \left[(\vec{\partial}^2 - \partial_0^2) \delta_{ij} - \partial_i \partial_j \right] \mathcal{A}_{j,u}. \quad (2.17)$$

The (un-rescaled) Coulomb and Lorentz gauge propagators are therefore given as $(\delta_{\text{tr}}^{ij}(\vec{k}) = \delta^{ij} - \frac{k^i k^j}{k^2}, \mathcal{G}_{\mu\nu}(k) = -(g_{\mu\nu} - (1 - \alpha) \frac{k_\mu k_\nu}{k^2 + i\epsilon}))$

	Coulomb gauge	Lorentz gauges	
soft:	$A_s^\mu : \text{---} \overset{\mu}{\text{---}} \overset{k}{\text{---}} \overset{\nu}{\text{---}} : \text{---}$	$\frac{i \delta_{\text{tr}}^{ij}(\vec{k})}{k^2 + i\epsilon}$	$\frac{i \mathcal{G}_{\mu\nu}(k)}{k^2 + i\epsilon},$
potential:	$A_{p,0} : \overset{0}{\text{---}} \overset{k, A_0}{\text{---}} \overset{0}{\text{---}} : \text{---}$	$\frac{-i}{-\vec{k}^2 + i\epsilon}$	$\frac{-i}{-\vec{k}^2 + i\epsilon},$
	$\vec{A}_p : \overset{i}{\text{---}} \overset{k, \vec{A}}{\text{---}} \overset{j}{\text{---}} : \text{---}$	$\frac{i \delta_{\text{tr}}^{ij}(\vec{k})}{-\vec{k}^2 + i\epsilon}$	$\frac{i [\delta^{ij} + (1 - \alpha) \frac{k_i k_j}{-\vec{k}^2 + i\epsilon}]}{-\vec{k}^2 + i\epsilon},$
ultrasoft:	$A_u^\mu : \text{---} \overset{\mu}{\text{---}} \overset{k}{\text{---}} \overset{\nu}{\text{---}} : \text{---}$	$\frac{i \delta_{\text{tr}}^{ij}(\vec{k})}{k^2 + i\epsilon}$	$\frac{i \mathcal{G}_{\mu\nu}(k)}{k^2 + i\epsilon}.$

(2.18)

The potential gluon becomes instantaneous in both gauges as expected for the particle mediating the Coulomb interaction. Insertions are necessary only in the potential régime:

	Coulomb gauge	Lorentz gauges	
$\overset{0}{\text{---}} \overset{k, A_0}{\text{---}} \text{---} \text{---} \overset{0}{\text{---}} :$	none	$-i \frac{k_0^2}{\alpha} = \text{P.C.}(v^2),$	
$\overset{i}{\text{---}} \overset{k, \vec{A}}{\text{---}} \text{---} \text{---} \overset{j}{\text{---}} :$	$i k_0^2 \delta_{ij} = \text{P.C.}(v^2)$	$i k_0^2 \delta_{ij} = \text{P.C.}(v^2),$	(2.19)
$\overset{i}{\text{---}} \overset{k, A^\mu}{\text{---}} \text{---} \text{---} \overset{0}{\text{---}} :$	none	$-i (1 - \frac{1}{\alpha}) k_i k_0 = \text{P.C.}(v)$	

The Lorentz gauge propagators and insertions for the potential and ultrasoft régimes were first given in [18]. Especially for the Feynman gauge $\alpha = 1$ ($\mathcal{G}_{\mu\nu}(k) = g_{\mu\nu}$), Lorentz and Coulomb gauges in the potential régime differ only by insertions, i.e. at higher order in v .

2.3 Vertex Rules

As an example, consider a bremsstrahlung-like process: the radiation of a soft scalar gluon $A_{s,0}$ off a soft quark, resulting in a potential quark with four momentum (T'_p, \vec{p}') . The rescaled interaction Lagrangean with its Hermitean conjugate reads

$$d^3X_s \, dT_s \left[-g \, v^0 \, \mathcal{Q}_s^\dagger(\vec{X}_s, T_s) \mathcal{A}_{s,0}(\vec{X}_s, T_s) \mathcal{Q}_p(\vec{X}_s, vT_s) + \text{H.c.} \right]. \quad (2.20)$$

The interaction Lagrangean is non-local in the rescaled variables, and in order to maintain velocity power counting, $\mathcal{Q}_p(\vec{X}_s, vT_s)$ has to be expanded about $\mathcal{Q}_p(\vec{X}_s, 0)$ in powers of v . The Feynman rule for this vertex is after inverting the rescaling

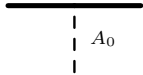





$$\begin{array}{c} \textcolor{red}{=} \\ \textcolor{black}{=} \end{array} \quad \begin{array}{c} (T, \vec{p}) \\ \textcolor{red}{\bullet} \end{array} \quad \begin{array}{c} (T'_p, \vec{p}') \\ \textcolor{black}{\bullet} \end{array} : -ig (2\pi)^4 \delta^{(3)}(\vec{p} - \vec{p}' + \vec{q}) \times \\ \times \left[\exp \left(-T'_p \frac{\partial}{\partial(T+q_0)} \right) \delta(T + q_0) \right] = \text{P.C.}(e^v) . \quad (2.21)$$

9

not resolve the precise time at which the soft quark emits or absorbs the soft gluon. This “temporal” multipole expansion comes technically from the different scaling of \vec{x} and t in the three régimes. The multipole expansion symbolised in the power counting by e^v corresponds term by term to an expansion in v and should be truncated at the desired order. In general, the coupling between particles of different régimes will not be point-like but contain multipole expansions for the particle belonging to the weaker kinematic régime. That the coupling of potential quarks to ultrasoft gluons requires a momentum multipole expansion as in atomic physics has been observed by Grinstein and Rothstein [19], and by Labelle [22].

Amongst the fields introduced, six scale conserving interactions are allowed within and between the various régimes for any coupling of one gluon to two quarks. Because only in the Coulomb gauge, A_0 is a field in the potential régime only, its propagator always being instantaneous, only the first two interactions exist for the scalar coupling $-gQ^\dagger A_0 Q$ of table 1 in this gauge choice. The v counting for the lowest order quark-gluon interactions from this vertex is presented in table 1.

Table 1: *Velocity power counting and vertices for the interaction Lagrangean $-gQ^\dagger A_0 Q$. In the Coulomb gauge, only the first two diagrams exist. The last line indicates the field for which an energy or momentum multipole expansion has to be performed.*

Vertex						
P.C.	$\frac{1}{\sqrt{v}}$	$v^{\frac{1}{2}}$	v^0	v^0	v^0	v
multipole	none	$A_p^0(\vec{x})$	$A_u^0(\vec{x})$	none	$Q_p(t)$	$A_u^0(\vec{x}, t)$

Note that – although both describing interactions with physical gluons – soft and ultrasoft couplings occur at different orders in v . On the level of the vertex rules, an overlap of different régimes resulting in double counting is prevented by the fact that in addition to most of the propagators, all vertices are distinct because of different multipole expansion rules.

This approach may be compared to power counting in loop diagrams as proposed in Beneke and Smirnov’s threshold expansion [16] where the strength of all scalar gluon interactions is v^0 because the scalar vertex $Q^\dagger A_0 Q$ of table 1 does not contain derivatives. Here, one can easily see that the Coulomb interaction is the only relevant coupling as $v \rightarrow 0$ and that it scales like $v^{-1/2}$. This follows immediately from the rescaling rules proposed. Also, the suppression of bremsstrahlung processes relative to the Coulomb interaction is evident from table 1. In threshold expansion, these features are established by considering scattering processes with an arbitrary number of loops.

Velocity power counting for other vertices is again obtained by rescaling and multipole

expansion. For later reference, the counting rules for the coupling of one and two gluons, either minimally or via the Fermi term, and the rules for the three gluon interaction are displayed in tables 2, 3 and 4. In the second, couplings between on shell gluons in the same régime are all of order $v^0 = c = 1$ as expected for relativistic particles.

In the minimal coupling term $-\frac{ig}{M} Q^\dagger \vec{\partial} \cdot \vec{A} Q$, the derivative acts on both the gluon and the quark field. Because the quark is either soft or potential, its derivative from $Q^\dagger \vec{A} \cdot \vec{\partial} Q$ is rescaled as $\vec{\partial} \rightarrow (Mv) \vec{\partial}_s$. The same holds when the derivative acts on a soft or potential gluon. But both for the one gluon part of the Fermi interaction $Q^\dagger \vec{\sigma} \cdot \vec{B} Q$ and for the term $Q^\dagger (\vec{\partial} \cdot \vec{A}) Q$ of the minimal coupling, the derivative acts on an ultrasoft gluon field and must hence be rescaled as $\vec{\partial} \rightarrow (Mv^2) \vec{\partial}_u$. That this part of the vertex coupling is one power in v weaker than the part where the derivative acts on the quark, is recorded in parentheses in table 2. The v rules for the coupling of one gluon to the quark via the Fermi term are identical to those sub-dominant contributions to the minimal coupling vertex for ultrasoft gluons, and to the dominant contributions in the other cases. A similar provision is made in table 3, but is not necessary in table 4.

Table 2: *Velocity power counting and vertices for the interaction $-\frac{ig}{M} Q^\dagger \vec{\partial} \cdot \vec{A} Q$. When the spatial derivative acts on an ultrasoft gluon field, the power counting in parentheses is the sub-dominant contribution as explained in the text. It coincides with the power counting for the one gluon component of the Fermi vertex.*

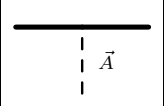
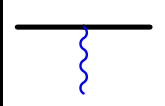
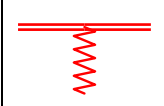
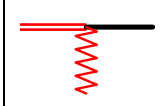

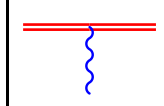

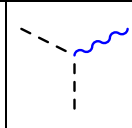
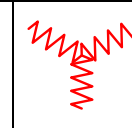
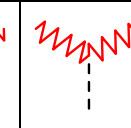
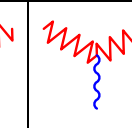
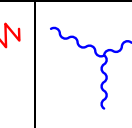
Vertex						
P.C.	$v^{\frac{1}{2}}$	$v \ (v^2)$	v	v	$v^{\frac{3}{2}}$	$v^2 \ (v^3)$

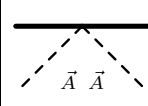
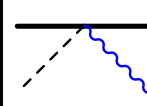
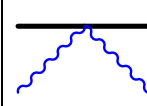
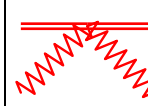
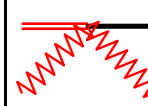
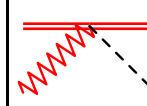
Table 3: *Velocity power counting and vertices for the gluonic interaction Lagrangean $\frac{g}{2} f^{abc} (\partial_\mu A_\nu^a - \partial_\nu A_\mu^a) A^{b,\mu} A^{c,\nu}$. Sub-dominant contributions in parentheses.*

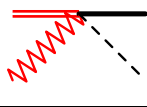
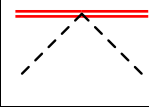

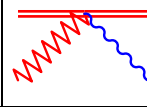
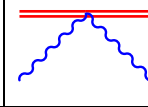
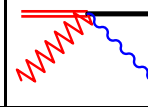
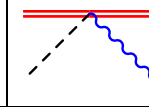
Vertex						
P.C.	$v^{\frac{1}{2}} \ (v^{\frac{3}{2}})$	$v \ (v^2)$	v^0	$v^{\frac{1}{2}} \ (v^{\frac{3}{2}})$	$v \ (v^2)$	v^0

2.4 Loop Rules

As hinted upon above, the velocity power counting is not yet complete. The propagators were constructed such that they count as order v^0 in each régime in a Feynman diagram.

Table 4: Velocity power counting and vertices for the coupling of two gluons to a quark from the minimal coupling or the Fermi term in the NRQCD Lagrangean (1.1).

Vertex						
P.C.	v	$v^{\frac{3}{2}}$	v^2	v	v	$v^{\frac{3}{2}}$

						
$v^{\frac{3}{2}}$	v^2	v	v^2	v^3	v^2	$v^{\frac{5}{2}}$

As one sees from the volume element used in (2.20), the vertex rules for the soft régime count powers of v with respect to the soft régime. There, one hence retrieves the velocity power counting of Heavy Quark Effective Theory [23, 24] (HQET), in which the interactions between one heavy (and hence static) and one or several light quarks are described. HQET counts inverse powers of mass in the Lagrangean, but because in the soft régime $Mv \sim \text{const.}$, the two approaches are actually equivalent. Now, HQET becomes a sub-set of NRQCD, complemented by interactions between soft (HQET) and potential or ultrasoft particles. This has already been used by Manohar [13] to facilitate and unify the matching of the NRQCD/HQET Lagrangean to QCD.

In NRQCD with on-shell quarks as initial and final states, the soft régime can occur only inside loops. Let us define as a “soft blob” each connected graph containing (soft) loops which is obtained when all potential and ultrasoft lines are cut. If the diagram contains even one soft particle, scale conservation ensures that there is at least one loop which consists of only soft particles, be they quarks or gluons, and that it is part of the soft blob. Inside the soft blob, the power counting for the vertices is performed in the soft régime and has therefore to be transferred to the potential régime. Since soft loop momenta scale like $[d^4k_s] \sim v^4$ while potential ones like $[d^4k_p] \sim v^5$, each soft blob is enhanced by an additional factor $\frac{1}{v}$.

Consider for example the graphs of Fig. 1: Using the Lorentz gauges, vertex power counting gives that the leading contribution is from the exchange of two potential gluons, coupled via $Q^\dagger A_0 Q$. There are four such vertices, so the diagram is $\mathcal{O}(g^4)$ P.C. (v^{-2}) from table 1. The next two diagrams are $\mathcal{O}(g^6)$ P.C. (v^0) and $\mathcal{O}(g^2)$ P.C. (v^1) from the vertex power counting in the soft régime, but another factor $\frac{1}{v}$ must be included because there is one soft blob in each diagram. This way, the v counting of the soft régime is moved to the potential one. The intermediate couplings in the second diagram take place in the

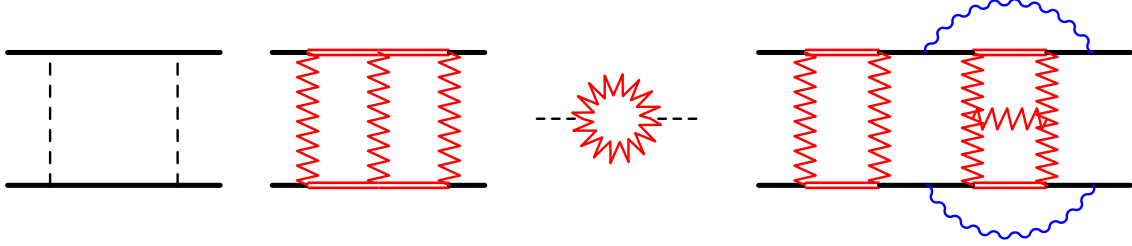


Figure 1: *Power counting with soft loops. The loops in the second and third diagram obtain an inverse power of v , the last diagram of v^2 in addition to the power counting following from the vertex rules.*

soft régime and hence are counted in that régime. After cutting all potential and ultrasoft lines in the last diagram, two soft blobs are separated by the propagation of two potential quarks. The graph is $\mathcal{O}(g^{14})$ P.C. (v^0) from the vertices, and the loop counting gives a factor $\frac{1}{v^2}$. Each soft blob contributes at least four powers of g , but only one inverse power of $v \sim g^2$. Power counting is preserved. These velocity power counting rules in loops are also verified in explicit calculations of exemplary graphs, [15] and App. A.2.

There is no similar rule for ultrasoft loops: In the absence of ultrasoft quarks (see Sect. 3.3), the internal ultrasoft gluon couples ultimately to a particle in the potential or soft régime. Those vertices are automatically counted in this stronger régime, while couplings between ultrasoft particles are counted in the weakest régime. No “ultrasoft blobs” can therefore be isolated by cutting all potential and soft lines. It is hence ultimately scale conservation which forbids a non-trivial loop counting rule for the ultrasoft régime.

Irrespective of the gauge chosen, there is only one relevant quark-gluon coupling at tree level in the renormalisation group approach (i.e. only one which dominates at zero velocity): As expected, it is the $Q_p^\dagger A_{p,0} Q_p$ coupling providing the binding (table 1). The potential gluon ladders must therefore be re-summed to all orders to yield the $\frac{1}{r}$ Coulomb potential. Diagrams higher order in v are corrections. In the Coulomb gauge, all other couplings and insertions are irrelevant, while in general, there are three marginal couplings: $Q_p^\dagger A_{u,0} Q_p$, $Q_s^\dagger A_{s,0} Q_s$ and $Q_s^\dagger A_{s,0} Q_p$. Because of the additional factor v^{-1} per soft blob, graphs containing the latter two couplings can indeed be relevant and contribute as $v \rightarrow 0$ (e.g. the second graph in Fig. 1). Eventually, retardation effects from A_p^μ will become weaker than contributions from the soft régime.

One finally turns to the inclusion of other relativistic particles. In the same way as NRQCD replaces the physical gluon with one representative per régime, any light (relativistic) particle has to be tripled. There are therefore three ghost fields η_s, η_p, η_u with the same rescaling rules as the gluon fields (2.6). Fermions require more thought: In the real world, the kinetic energy of the b quark in Bottomium is compatible to the strange quark mass, $M_b v^2 \sim m_s$. For the sake of simplicity, this article assumes all light particles to have masses very much smaller than any other scale, $m_q \ll M v^2$, so that the relativistic particles can be treated as massless to lowest order and the denominators of the light particle propagators are identical to the ones of the gluon in the respec-

tive régimes. The Dirac spinors representing light quarks scale in the three régimes as $\psi_s \sim (Mv)^{\frac{3}{2}} \sim \psi_p, \psi_u \sim (Mv^2)^{\frac{3}{2}}$, i.e. similar to the heavy quark but including its ultrasoft counterpart (see also Sect. 3.3). The number of vertices per term in the rescaled interaction Lagrangean increases as shown above. Quark-ghost couplings and heavy-light quark couplings will appear in the Lagrangean (1.1) at $\mathcal{O}(g^4)$ to restore unitarity and can be obtained by matching NRQCD to QCD.

With rescaling, multipole expansion and loop counting, the velocity power counting rules are established. To witness, the rescaling rules (2.5/2.6/2.7) provide an efficient and well-defined way to arrive at an NRQCD power counting: After rescaling, one reads up the order in v at which any term in the Lagrangean contributes in each of the three kinematic régimes and performs the appropriate multipole expansions. This establishes the Feynman rules for NRQCD and HQET simultaneously, and classifies the strength of the vertices in the régime of the particle with highest energy and momentum. Finally, the rescaling is inverted, introducing one un-rescaled gluon and quark field as the infrared-relevant degrees of freedom for each kinematic régime. To obtain the power counting for a certain graph, loop counting is taken into account to transfer the strength of a soft blob into the potential régime. Computations are performed most naturally in the original, dimensionful variables. The rescaling rules are only needed to establish the power counting, but in order to maintain it, one is of course not allowed to re-sum the multipole expansions in the un-rescaled variables. It is also interesting to note that there is no choice but to assign one and the same coupling strength g to each interaction. Different couplings for one vertex in different régimes are not allowed. This is to be expected, as the fields in the various régimes are representatives of one and the same non-relativistic particle, whose interactions are fixed by the non-relativistic Lagrangean (1.1).

2.5 Gauge Invariance

The Coulomb gauge $\vec{\partial} \cdot \vec{A} = 0$ is a natural choice in NRQED because in it, static charges do not radiate. In NRQCD, gluons carry colour and hence the Coulomb gauge does not have this advantage. Luke and Savage [18] showed how to establish explicit velocity power counting in the Lorentz gauges of NRQCD, too. The set of gauges applicable to NRQCD can be extended further: The classification of the three kinematic régimes (2.2) itself relied only on the typical excitation energy and momentum, and hence on gauge invariant quantities, and on the form of the denominator in the propagators (2.1) which is unchanged in any order of perturbation theory³. The perturbative quark propagator is gauge independent. Gauge fixing will introduce gauge dependent denominators multiplying the gauge independent denominators in the perturbative gluon propagators. As an example that this will in general not change the identification of the soft and ultrasoft régimes from poles in the gluon propagators, consider the generalised axial gauge

³Non-perturbatively, the propagators are not of the form (2.1) because of confinement and the absence of coloured states, so that the power counting presented here may break down.

($n^2 = -1$, α arbitrary), in which

$$A^\mu : \frac{-i}{k^2 + i\epsilon} \left[g_{\mu\nu} - \frac{k_\mu n_\nu + n_\mu k_\nu}{k \cdot n} + \frac{1 + \alpha k^2}{(n \cdot k)^2} \right] . \quad (2.22)$$

The additional denominators $n \cdot k$ introduce no new combinations of the two infrared scales Mv and Mv^2 for which the gluon propagator has a pole. Therefore, the decomposition into the three régimes (2.2) remains unchanged, as do the rescaling properties of the fields and interactions, (2.5/2.6/2.7) and tables 1 to 4.

The standard gauges (axial, Weyl, Lorentz, Coulomb) will therefore all show the same power counting and vertex rules quoted above. Details of the gluon propagator and its insertions look different in different régimes and gauges, and some gauges will not exhibit certain vertices, insertions and representatives, e.g. the Coulomb gauge is unique in having A_0 contribute only in the potential régime. Only when the gauge dependent denominator introduces a new régime has the power counting to be modified. This is for example the case in a gauge with denominator $k_0^4 - M^2 \vec{k}^2$, in which an exceptional régime ($k_0 \sim Mv$, $|\vec{k}| \sim Mv^2$) enters. Rescaling is then performed including the new régime.

As is well known, the Weyl gauge $A_0 = 0$ wants a constraint quantisation: Gauß' law $\vec{D} \cdot \vec{E} = gQ^\dagger Q$, generating local gauge transformations, is the equation of motion derived by varying the Lagrangean with respect to A_0 . When $A_0 = 0$, Gauß' law will not be recovered as an equation of motion. In order to restore local gauge invariance, a projector onto states obeying Gauß' law has therefore to be inserted into the path integral. Resolving Gauß' law explicitly, the Lagrangean of the Coulomb interaction has the structure

$$\mathcal{L}_{\text{Coulomb}} = \int d^3y \, g^2 \, Q^\dagger Q(\vec{x}) \, \mathcal{G}(\vec{x} - \vec{y}) \, Q^\dagger Q(\vec{y}) , \quad (2.23)$$

where $\mathcal{G}(\vec{x} - \vec{y})$ is an appropriate instantaneous Green's function to Gauß' law with dimension $[\text{mass}]^1$, e.g. in QED $\frac{1}{|\vec{x} - \vec{y}|}$. Using the rescaling rules (2.5/2.6/2.7), one derives the Coulomb interaction between two quarks to be P.C. (v^{-1}) as in the other gauges. Without constraint quantisation, the longitudinal component of the vector gauge field mediating the Coulomb interaction in Weyl gauge QED, \vec{A}^l , has a static propagator $\frac{i}{k_0^2}$.

3 The NRQCD β Function

This chapter presents the computation of the perturbative part of the NRQCD β function to order g^3 , v^0 in the $\overline{\text{MS}}$ scheme using the vertex and rescaling rules derived in the previous section. Initially, the Lorentz gauges are not only chosen because they allow a less cumbersome renormalisation than e.g. the Coulomb gauge, but also to demonstrate that in the final result, the gauge parameter α drops out. The Slavnov–Taylor identities will be shown to be fulfilled, and the Lorentz gauges are a legitimate gauge choice in NRQCD. As a by-product, Sect. 3.7 will calculate the NRQCD β function to lowest order in the Coulomb gauge.

By construction, NRQCD and QCD must agree in the infrared limit, and especially in the structure of collinear (infrared) divergences. Matching proved that both the soft

quark and the soft gluon are indispensable to reproduce the correct structure of collinear divergences in a toy model given by Beneke and Smirnov [16] and confirmed the proposed counting rules [15]. The calculation of the NRQCD β function will manifest the relevance of the soft régime beyond infrared divergences, and it will endorse the power counting further. Deriving the lowest order β function in the following, the relation between this power counting and threshold expansion [16] will be exemplified, and rules will be developed which allow one to determine from the structure of a diagram whether it is zero or not to all orders in v .

NRQCD with N_F light quarks must reproduce the β function of QCD below the scale M ,

$$\beta_{\text{QCD}} = - \frac{g_R^3}{(4\pi)^2} \left[\frac{11}{3} N - \frac{2}{3} N_F \right] \quad (3.1)$$

to lowest order for the gauge group $SU(N)$ and renormalised coupling g_R . This means especially that the renormalised coupling strengths of all interactions stemming from expanding the same term in the Lagrangean in the various régimes are the same, except that they have to be taken at different scales: For the interaction Lagrangean $-gQ^\dagger A_0 Q$, the six vertices of table 1 all couple with the same un-renormalised strength. Although the number of vertices is increased in the approach presented here, the number of independent couplings is not. Indeed, one major result of this chapter will be that renormalisation will not destroy this symmetry because the renormalisation constants agree in all régimes.

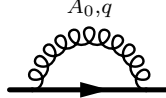
One can obtain the β function from the ghost-gluon coupling, and the ghost and gluon self energy. Because the relativistic sector of NRQCD is identical to the one of QCD as seen in Sect. 2.3, the calculation proceeds in that case like in QCD and yields the same result. In this article, the β function is calculated by studying the heavy quark sector, namely the renormalised coupling $Q_R^\dagger A_{0,R} Q_R$ between the heavy quark and the scalar gluon. This term yields immediately the coupling renormalisation. All other vertices are suppressed by at least one power of v .

Because the integrals to be performed are not Lorentz invariant, standard formulae for dimensional regularisation often do not apply. Therefore, Ref. [15] used split dimensional regularisation, which was introduced by Leibbrandt and Williams [25] to cure the problems arising from pinch singularities in non-covariant gauges. It treats the temporal and spatial components of the loop integrations on an equal footing by regularising the energy and momentum integration separately, $\int \frac{d^d k}{(2\pi)^d} = \int \frac{d^\sigma k_0}{(2\pi)^\sigma} \frac{d^{d-\sigma} \vec{k}}{(2\pi)^{d-\sigma}}$, $\sigma \rightarrow 1$, $d \rightarrow 4$ [26, Chap. 4.1]. Useful formulae for the computation of the β function are given in App. A.1.

3.1 NRQCD and Threshold Expansion: Potential Quark Self-Energy

Threshold expansion [16] and NRQCD make use of very similar basic techniques but different formulations, as this Section outlines. In order to clarify the relation, consider the quark self-energy diagram lowest order in g which couples the scalar gluon and the quark in NRQCD. To facilitate the presentation initially, the Feynman gauge $\alpha = 1$ is

chosen in which scalar and vector gauge fields do not mix when propagating. Without the scaling rules for the various régimes, one obtains



$$: i\Sigma_p(T, \vec{p}) = (-ig)^2 C_F \int \frac{d^d q}{(2\pi)^d} \frac{-i}{q_0^2 - \vec{q}^2 + i\epsilon} \frac{i}{T + q_0 - \frac{(\vec{p} + \vec{q})^2}{2M} + i\epsilon}, \quad (3.2)$$

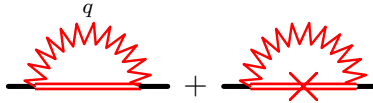
with $C_F \delta_{ij} = (t^a t^a)_{ij} = \frac{N^2 - 1}{2N} \delta_{ij}$ the Casimir operator of the fundamental representation of $SU(N)$. Threshold expansion identifies the loop momentum of QCD to belong to a hard régime $q \sim M$ or to either of the three régimes (2.2) and expands the integrand about the various saddle points, i.e. about the values of the loop-momentum q where poles occur, like the NRQCD classification in Sect. 2.1. The hard régime subsumes the relativistic effects contained in the coefficients c_i, d_i, e_i of the NRQCD Lagrangean (1.1) and hence provides the matching between NRQCD and QCD [16]. In deriving the NRQCD Lagrangean (1.1), hard momenta have been integrated out, so that the ultraviolet behaviour of the above loop integral is arbitrary and it is not necessary to take the poles at $q \sim M$ in (3.2) into account. Indeed, to be consistent, they should rather be discarded.

Let the incident quark be on shell, i.e. have a four-momentum (T_p, \vec{p}) in the potential régime. The integral decomposes then into approximations about three saddle points: When q is soft, the gluon propagator has a pole, and one can expand the quark propagator in powers of $T_p/q_0 \sim v$ and $\frac{(\vec{p} + \vec{q})^2}{2M}/q_0 \sim v$. The quark becomes static:

$$\frac{i}{q_0 + T_p - \frac{(\vec{p} + \vec{q})^2}{2M}} \longrightarrow \frac{i}{q_0} + \frac{i}{q_0} i \left(T_p - \frac{(\vec{p} + \vec{q})^2}{2M} \right) \frac{i}{q_0} + \dots \quad (3.3)$$

$$\Rightarrow i\Sigma_p(T, \vec{p})|_{\text{soft}} = (-ig)^2 C_F \int \frac{d^d q}{(2\pi)^d} \frac{-i}{q_0^2 - \vec{q}^2 + i\epsilon} \frac{i}{q_0 + i\epsilon} \sum_{n=0}^{\infty} \left(\frac{\frac{(\vec{p} + \vec{q})^2}{2M} - T_p}{q_0 + i\epsilon} \right)^n \quad (3.4)$$

The NRQCD power counting proceeds on the level of the Lagrangean instead of the Feynman diagrams with corresponding diagrams for loop momenta in the soft régime,



$$+ \dots : \quad (3.5)$$

$$(-ig)^2 C_F \int \frac{d^d q}{(2\pi)^d} \frac{-i}{q_0^2 - \vec{q}^2 + i\epsilon} \frac{i}{q_0 + i\epsilon} \left(1 - i \frac{(\vec{p} + \vec{q})^2}{2M} \frac{i}{q_0 + i\epsilon} + iT_p \frac{i}{q_0 + i\epsilon} + \dots \right),$$

and recovers order by order in v the result of threshold expansion. The intermediate soft quark is static, and the higher order terms in threshold expansion are interpreted as insertions into the soft quark propagator or as resulting from the energy multipole expansion at the $Q_s A_s^\mu Q_p$ vertex. In fact, using the equations of motion, a temporal multipole expansion may be re-written such that the energy becomes conserved at the vertex. Now, both soft and potential or ultrasoft energies are present in the propagators,

The important step to cut down the computational effort in either approach is to note that as an immediate consequence of the axioms of dimensional regularisation (e.g. [26, Chap. 4.1 and 4.2]), integrals without scales set by external momenta or energies in the denominator vanish because of homogeneity,

$$\int \frac{d^d q}{(2\pi)^d} q^\alpha = 0 \quad . \quad (3.10)$$

For example, applying this theorem to the potential quark self energy diagrams, contributions from soft (3.4) and potential (3.8) loop momenta are zero to all orders in the velocity expansion. For the potential gluon contribution (3.8), this is seen by shifting the regularised loop integral $T + q_0 - \frac{(\vec{p}+\vec{q})^2}{2M} \rightarrow q_0$ before using (3.10) for the energy integral. The importance of (3.10) has already been alluded to in threshold expansion [16], and here a more thorough and formal treatment is presented.

It is this theorem (3.10) which renders most of the diagrams in NRQCD and threshold expansion calculations zero, and it is usually not even necessary to consider the whole diagram but only a sub-set of it. The following set of rules is helpful for reducing the numbers of diagrams to be dealt with in the calculation of the β function.

In order to establish these rules, recall that all graphs vanish which contain a sub-graph zero by the rules developed. The routing of the loop four-momentum inside a diagram is arbitrary as always in dimensional regularisation so that having regularised the loop integration, all loop four-momenta can be shifted at will like in ordinary integration. Since they have identical denominators (Sect. 2.3), gluon lines in any rule can be replaced by any relativistic particle, e.g. ghosts and light quarks. Finally and most importantly, numerators are unimportant to determine whether an integral is scale-less following (3.10). As multipole expansion and insertions do not change the denominators of the propagators, a diagram is therefore zero to all orders when it is zero because of (3.10) at leading order in v . This result is also insensitive to the gauge chosen and to the specific vertex involved. For example, because the numerators play no rôle in rendering (3.4/3.8) zero using (3.10), the same will hold for any graph with the same diagrammatic representation but different interactions, e.g. also for graphs in which one or both vertices are replaced with the minimal coupled vector fields $Q^\dagger \vec{\partial} \cdot \vec{A} Q$ or the Fermi interaction $Q^\dagger \vec{\sigma} \cdot \vec{B} Q$.

As a first rule, consider a potential gluon between two soft particles, represented by the overlay of double and zigzag lines in Fig. 2 (a). This sub-diagram is zero when the loop energy q_0 is integrated over: Assign the potential loop momentum q to the instantaneous gluon with a propagator denominator $-\vec{q}^2$ (2.18). As the coupling of soft particles to potential ones is energy non-conserving, the denominators of the soft particles coupling to A_p^μ do not contain $q_0 \sim Mv^2$, either. Therefore, q_0 does not occur in any denominator, and the dimensionally regularised loop integral over q_0 is zero from (3.10). The rule is extended by noting (Fig. 2 (b)) that overall energy conservation allows for the potential gluon line to be attached with an arbitrary number of vertices into which an arbitrary number of potential or ultrasoft gluons or quarks with collective (potential) four-momentum l enters.

for its bare and (b) for its dressed form. The vertices are again energy non-conserving, so

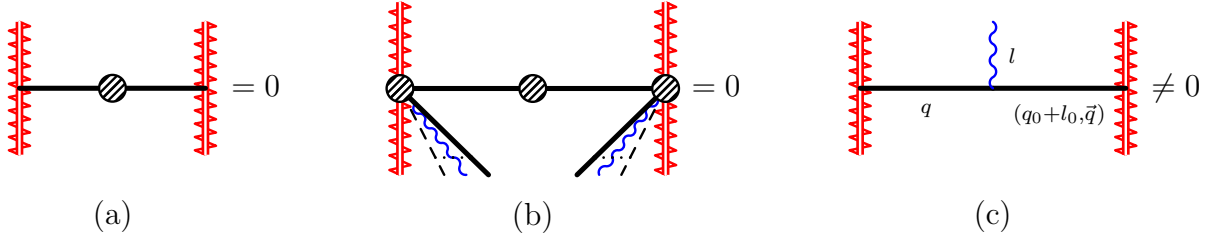


Figure 3: *The second rule in its bare (a) and dressed (b) version; (c) the generalisation analogous to Fig. 2 (c) fails. Conventions as in Fig. 2.*

that q_0 enters only in the denominator of the potential quark in the combination $q_0 - \frac{\vec{q}^2}{2M}$. Shifting $q_0 - \frac{\vec{q}^2}{2M} \rightarrow q_0$, the q_0 integral again does not contain a scale in the denominator. In contradistinction to the previous case, this rule cannot be extended to include potential or ultrasoft momenta coupling to the blob, Fig. 3 (c). For example, a bremsstrahlung gluon with external, ultrasoft four-momentum l renders the potential quark denominators in the propagators as $(q_0 - \frac{\vec{q}^2}{2M})(q_0 + l_0 - \frac{\vec{q}^2}{2M})$. Now, l_0 provides the necessary scale for the q_0 integration. As an example of the rule, the Abelian vertex contribution with denominator

$$(T, \vec{p}) \quad \text{---} \quad \text{---} \quad (T', \vec{p}') \quad : \text{Denom.} = \left(q_0 - \frac{\vec{q}^2}{2M} \right) (T - T') (T'^2 - (\vec{p}' - \vec{q})^2) \quad (3.12)$$

is zero, but the last of the graphs in Fig. 1 is not.

As the coupling of an ultrasoft gluon to a soft particle conserves neither energy nor momentum, one may disconnect the ultrasoft gluon from such a vertex, Fig. 4 (a). If after

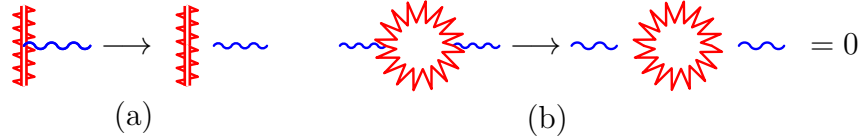


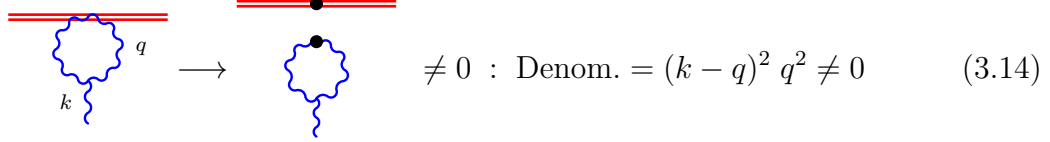
Figure 4: *(a) Soft-to-ultrasoft vertices are cut off in a third rule; (b) an example. Conventions as in Fig. 2.*

cutting, a line with loop momenta to be integrated over becomes completely disconnected from the graph, the resulting tadpole makes the graph vanish, Fig. 4 (b). If only one of the A_μ^u legs becomes dis-attached, the diagram can be non-zero, as the following diagram for the Abelian vertex correction to the $Q_s A_{s0} Q_p$ coupling demonstrates:

$$(T, \vec{p}) \quad \text{---} \quad \text{---} \quad (T', \vec{p}') \quad \longrightarrow \quad \text{---} \quad \text{---} \quad \neq 0 : \text{Denom.} = T q^2 \left(T' - q_0 - \frac{\vec{p}^2}{2M} \right) \quad (3.13)$$

See also Sect. 3.6 and the computation of this graph in App. A.2.

When several ultrasoft gluons couple to a soft particle at the same point, cutting does usually not result in a tadpole, either. For example, the gluon-gluon vertex obtained by cutting the two-gluon two-quark vertex



$$\neq 0 : \text{Denom.} = (k - q)^2 q^2 \neq 0 \quad (3.14)$$

might be represented by a small blob as a reminder that it is neither energy nor momentum conserving. In the “tadpole”, a scale is set by the external ultrasoft four-momentum k .

Loops made out of one soft quark and one soft gluon are restricted by another rule. In

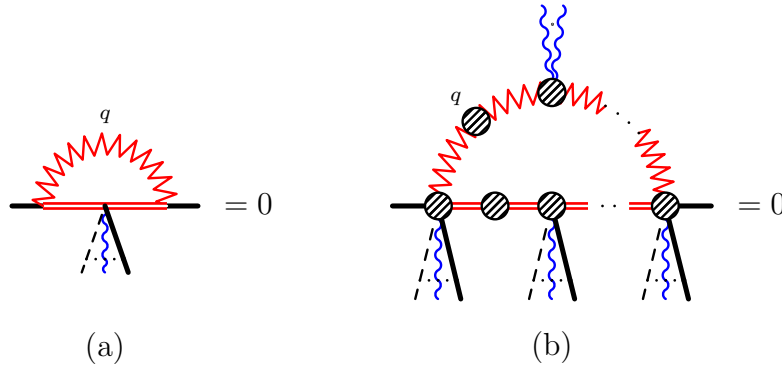
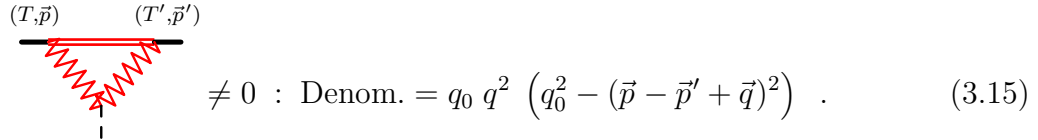


Figure 5: The fourth rule in its (a) bare and (b) extended version, where the rule in Fig. 4 (a) was used for attaching ultrasoft gluons to the soft gluon. Conventions as in Fig. 2.

Fig. 5 (a), the denominators are $q_0^2 - \vec{q}^2$ for the soft gluon and q_0 for the soft quark. Therefore, the diagram is without scale. The generalisation, Fig. 5 (b), eliminates all soft contributions to the potential quark self energy (3.5) and to Abelian vertex corrections between potential and ultrasoft particles. Note that the light particle exchanged is massless or has a mass considerably smaller than Mv^2 . A relativistic particle mass of order Mv^2 or bigger provides a scale in the relativistic propagator, invalidating this rule. Also, as soon as a potential particle couples to the soft gluon, the diagram is non-zero. An example is the non-Abelian vertex correction to the $Q_p^\dagger A_p^\mu Q_p$ coupling with denominator



$$\neq 0 : \text{Denom.} = q_0 q^2 \left(q_0^2 - (\vec{p} - \vec{p}' + \vec{q})^2 \right) \quad (3.15)$$

To summarise, the principle underlying the rules is simple: One identifies a potentially vanishing sub-set of the entire diagram and assigns the external and loop momenta to it, taking into account multipole expansions. Then, the denominators (i.e. inverse propagators) are written out at lowest order in v . If by shifting integration variables, one arrives

(denoted by a dotted line) is static because $T \sim Mv^2$, $|\vec{p}| \sim Mv^2$,

$$Q_u : \cdots \cdots \cdots \text{blue triangle} \cdots \cdots \cdots : \frac{i}{T + i\epsilon} ; \quad (3.18)$$

and that it couples momentum non-conserving to all but ultrasoft particles. These features can of course be derived from the rescaling rules of an ultrasoft quark, $Q_u(\vec{x}, t) = (Mv^2)^{\frac{3}{2}} \mathcal{Q}_u(\vec{X}_u, T_u)$, in full analogy to Sect. 2.2. If it exists, Q_u can only enter in internal lines. Fermion number conservation dictates that it is produced and annihilated in a vertex into which at least one soft or potential quark enters.

The simplest sub-diagram containing an ultrasoft quark is depicted in Fig. 7 (a) and vanishes because there is no loop momentum \vec{q} in any denominator. This is still true

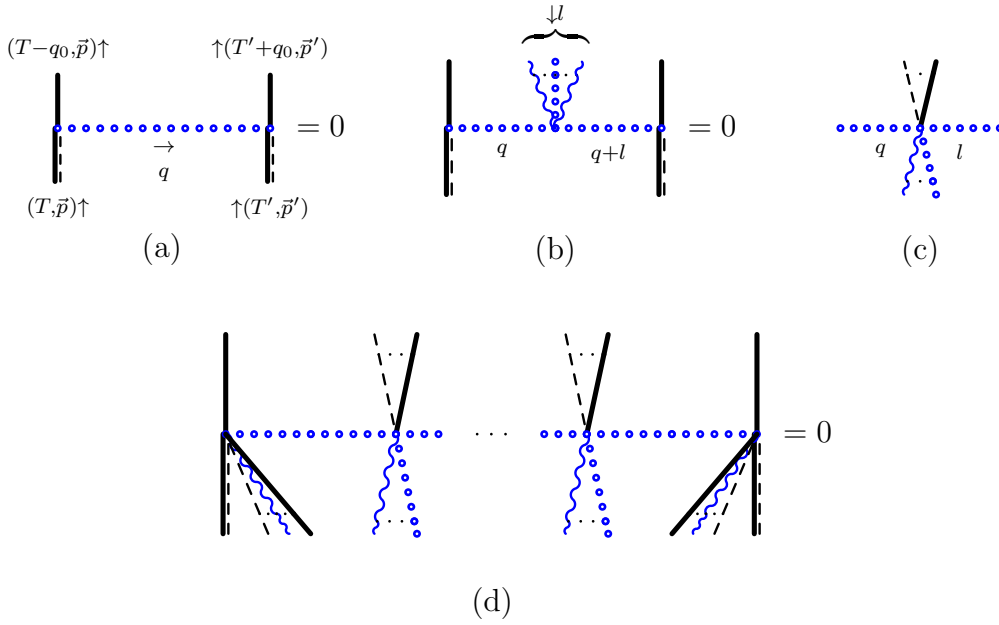
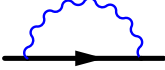


Figure 7: *Decoupling of the heavy, ultrasoft quark. (a) primitive diagram; (b) extension to the case of ultrasoft particles coupling to Q_u ; (c) general vertex involving potential and ultrasoft particles; (d) ultrasoft quarks decouple from any graph containing potential and ultrasoft particles. Conventions as in Fig. 2.*

when an arbitrary number of ultrasoft particles couple to Q_u , Fig. 7 (b), and when such a coupling occurs repetitively. Now one considers couplings to potential particles like in Fig. 7 (c). The momentum multipole expansion necessary for all ultrasoft particles separately in such a vertex disallows \vec{q} to be transferred to a denominator. Therefore, any diagram containing an ultrasoft quark coupled to potential or ultrasoft particles is zero because of the spatial tadpole in the q integration, Fig. 7 (d). Because couplings of ultrasoft particles to soft ones involve the same momentum multipole expansion as couplings to potential ones, the proof extends to all graphs containing ultrasoft quarks: Every diagram with ultrasoft quarks is zero. Recursive application dresses all vertices and propagators.

3.4 The Quark Self-Energy

The rules cover the lowest order contributions to the potential quark self energy as discussed in Sect. 3.1. The graph in (3.5) is zero because of Fig. 5, the one in (3.8) because of forwardness. The only remaining graph is (3.9), whose lowest order contribution is P.C.(v^0) by the power counting of table 1. Indeed, corrections to particle propagators, quark or gluon, must count as v^0 since the power counting was constructed such that free particle propagators in each régime scale like v^0 (2.6/2.7) and renormalisation corrections to propagators must be of the same order. Using the integral (A.4) of App. A.1, the pole in four dimensions is extracted as




$$: i\Sigma_p(T, \vec{p})|_{\text{pole}} = \frac{-ig_R^2 \mu^{2\varepsilon}}{8\pi^2} C_F \frac{3-\alpha}{2} \Gamma[\varepsilon] \left(T - \frac{\vec{p}^2}{2M} \right) + \text{P.C.}(v) \quad , \quad (3.19)$$

where $\varepsilon = 2 - \frac{d}{2}$ and μ is the renormalisation parameter. The potential quark propagator is recovered, confirming that different régimes do not mix under renormalisation. The non-relativistic quark propagator does not need renormalisation of the heavy quark mass. The quark wave function renormalisation is hence in the MS scheme

$$Z_2 = 1 + \frac{g_R^2 \mu^{2\varepsilon}}{8\pi^2} C_F \frac{3-\alpha}{2} \Gamma[\varepsilon] \quad . \quad (3.20)$$

For the soft quark self energy, the only diagram surviving the diagrammatic filter (Fig. 6) is at lowest order in the power counting using the Feynman rules and (A.4)



$$: i\Sigma_s(T, \vec{p})|_{\text{pole}} = \frac{-ig_R^2 \mu^{2\varepsilon}}{8\pi^2} C_F \frac{3-\alpha}{2} \Gamma[\varepsilon] T \quad . \quad (3.21)$$

That the soft quark renormalisation is the same as for the potential quark is not surprising as both stem from the same un-expanded NRQCD diagram (3.2).

3.5 The Vacuum Polarisation

In contradistinction to the self energy for Q_p which does not receive contributions from soft particles, the vacuum polarisation of the potential gluon is non-zero only because of the presence of soft gluons, independent of the gauge chosen. The scale-conserving graphs with gluon loops are




$$\quad \quad \quad (3.22)$$

The integral in the second graph does not contain q_0 in the denominator and hence is zero; the third diagram vanishes because it couples a potential gluon to a light-like particle twice. Soft gluons are therefore indispensable to provide the gluons mediating

the Coulomb interaction with a non-zero vacuum polarisation, and hence to have a running β function. As the gluons in the soft and ultrasoft régimes are on-shell particles and must run in NRQCD as in QCD, there is no reason to expect the potential gluons to freeze out in perturbation theory. The only non-zero ghost and light quark contributions come analogously from soft ghost and soft light quark propagation in the loop.

The rescaling rules of table 3 give the three gluon vertex to count as $v^{\frac{1}{2}}$, and an additional v^{-1} from the loop power counting makes the graph count as v^0 at leading order. Again, this is expected not only because gluons are relativistic particles, but also because one wants to renormalise a propagator which is P.C.(v^0) in the power counting. Without the loop rule of Sect. 2.4, the graph would be of order v^1 , and the power counting would predict that its contribution would vanish as $v \rightarrow 0$ so that the potential gluon propagator at rest would reduce to the bare one, a clearly unacceptable conclusion. The explicit computation (3.24) will also show that this graph is P.C.(v^0).

The soft and ultrasoft gluon receive their vacuum polarisations from loops with on shell gluons, P.C.(v^0):


(3.23)

All other diagrams vanish by the rules developed above. Both contributions are identical to the ordinary QCD result, as no insertions or expansions enter. The gluon vacuum polarisation from gluon, ghost and light fermion contributions is therefore in the soft and ultrasoft régime [27, eq. (2.5.132)]

$$\begin{aligned} \Pi_{\mu\nu}^{ab}(k) &= \delta^{ab} (k_\mu k_\nu - k^2 g_{\mu\nu}) \Pi(k^2) \quad \text{with} \\ \Pi(k^2) &= \frac{g_R^2 \mu^{2\varepsilon}}{(4\pi)^2} \left[\frac{2}{3} N_F - \frac{1}{2} N \left(\frac{13}{3} - \alpha \right) \right] \Gamma[\varepsilon] + \text{finite}. \end{aligned} \quad (3.24)$$

Because the potential gluon vacuum polarisation does not contain insertions or multipole expansions in the internal lines, either, the QCD result can be taken and expanded in powers of the external energy $k_0 \ll |\vec{k}|$. As the infinite part of $\Pi(k^2)$ does not contain k , the only change will be that to lowest order in v , the part guaranteeing transversality of the gluon becomes

$$(k_\mu k_\nu - k^2 g_{\mu\nu}) \rightarrow (\delta_{\mu i} \delta_{\nu j} k_i k_j + \vec{k}^2 g_{\mu\nu}) + \text{P.C.}(v) \quad . \quad (3.25)$$

Renormalisation therefore keeps the contributions from the three régimes separate and the potential gluon propagator transversal up to higher order in v . For all three régimes, the gluon wave function renormalisation is in the end the one of QCD [27, eq. (2.5.135)],

$$Z_3 = 1 - \frac{g_R^2 \mu^{2\varepsilon}}{(4\pi)^2} \left[\frac{2}{3} N_F - \frac{1}{2} N \left(\frac{13}{3} - \alpha \right) \right] \Gamma[\varepsilon] = Z_3^{\text{QCD}} \quad . \quad (3.26)$$

3.6 The Vertex Correction and NRQCD β Function

Since they probe only the relativistic sector of the theory, the renormalisation constants for gluons, ghosts and other light particles are the same in QCD and NRQCD. The quark wave function renormalisation is computed in the non-relativistic sector and for a non-relativistic bi-spinor rather than a relativistic Dirac spinor, so that it is not surprising that the result (3.20) differs from its QCD counterpart $Z_2^{\text{QCD}} = 1 - \frac{g_R^2 \mu^{2\varepsilon}}{(4\pi)^2} C_F \alpha \Gamma[\varepsilon]$ [27, eq. (2.5.139)] even in the dependence on α , although the $\overline{\text{MS}}$ scheme was used in both cases. As both Lagrangeans are gauge invariant and agree in the light particle sector, the Slavnov–Taylor identities of QCD must also hold in NRQCD. Therefore, the renormalisation Z_1 of the quark-gluon vertex $Q^\dagger A_0 Q$ can be inferred from Z_2, Z_3 and the three-gluon renormalisation $Z_{1,g}$ of QCD (and NRQCD) not to be the same as in QCD where $Z_1^{\text{QCD}} = 1 - \frac{g_R^2 \mu^{2\varepsilon}}{8\pi^2} (C_F \alpha + N \frac{3+\alpha}{4}) \Gamma[\varepsilon]$ [27, eq. (2.5.145)]:

$$Z_1 = \frac{Z_2 Z_{1,g}}{Z_3} = 1 + \frac{g_R^2 \mu^{2\varepsilon}}{(4\pi)^2} \left(C_F (3 - \alpha) - N \frac{3 + \alpha}{4} \right) \Gamma[\varepsilon] \neq Z_1^{\text{QCD}}. \quad (3.27)$$

In the following, one will identify as the cause that all non-zero contributions from both Abelian and non-Abelian vertex corrections to the scalar gluon vertex in NRQCD are different from their QCD values: Most notably, the non-Abelian vertex only provides gauge parameter corrections. As a by-product, the topologies of all one loop corrections to interactions of one gluon with a quark will be found and their leading order velocity power counting determined.

Which vertices may be encountered in the graphs leading in v ? For every vertex, the $Q^\dagger A_0 Q$ coupling is at least one order stronger in v than any other coupling (tables 1 and 2). Any contribution is therefore suppressed in which scalar gluons in a vertex are replaced with vector gluons, coupled either minimally or via the Fermi term $\frac{g c_3}{2M} Q^\dagger \vec{\sigma} \cdot \vec{B} Q$ in (1.1). Moreover, the Fermi term couples one or two gluons to the quark spin. When only one Fermi interaction is found in any vertex correction, parity conservation requires the strongest possible correction involving A_0 as outgoing particle to be of the form of the spin-orbit term, i.e. proportional to $Q^\dagger \vec{\sigma} \cdot (\vec{D} \times \vec{E}) Q$. This cannot correct the leading scalar gluon vertex. Two Fermi interactions are even more suppressed because vector couplings are weaker than scalar couplings.

Each Abelian correction graph (Fig. 8) starts off at the same order as the bare graph whose vertex correction it presents (table 1) when only scalar gluons couple to the quark. The only exception is the last diagram in the first row of Fig. 8, which by the power counting is P.C.(v^1) while the bare $Q_s^\dagger A_{s0} Q_p$ vertex is P.C.(v^0) from table 1, as confirmed by an explicit computation of this graph in App. A.2. This diagram does therefore not enter in the computation of the vertex correction at lowest order.

The non-Abelian corrections to the $Q^\dagger A_0 Q$ vertex at order g^3 fall into two categories: The topology of the first class of diagrams, Fig. 9, is analogous to the one of the non-Abelian vertex correction in QCD. In the Feynman gauge $\alpha = 1$, its leading order contribution involves two scalar gluons and one vector gluon because in that gauge, different components of the gluon field do not mix when propagating, (2.18), and the coupling of

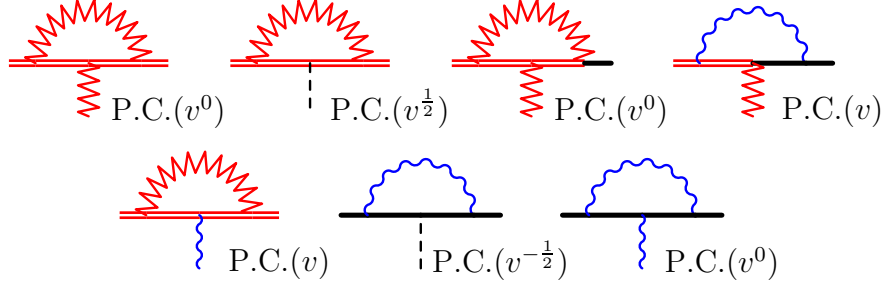


Figure 8: The Abelian vertex corrections of order g^3 from the interactions $Q^\dagger A_0 Q$ which survive the diagrammatic filter. The leading order power counting is obtained when all vertices are the leading order scalar gluon interactions. After applying the rules of Sect. 3.2, the seven diagrams drawn are the only survivors of 22 scale conserving graphs.

three scalar gluons is forbidden at order g by the Lorentz structure. Again because for

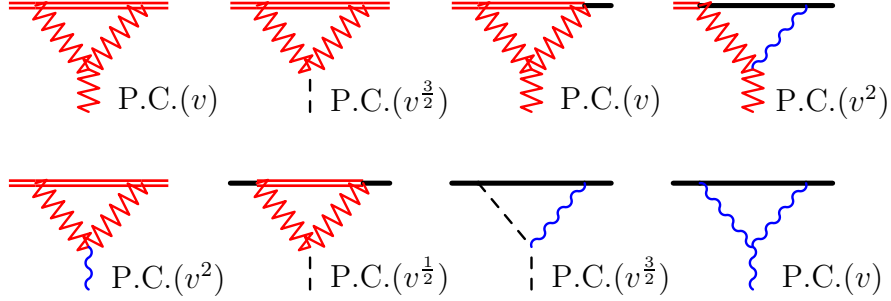


Figure 9: The non-Abelian vertex corrections of order g^3 which survive the diagrammatic filter. The soft blob in the second diagram in the second row provides an additional factor $\frac{1}{v}$ by loop power counting. The power counting indicated is the leading contribution in the Feynman gauge, when the three gluon vertex is the standard QCD one and both one vector and one scalar gluon couples minimally to the quark. In the Lorentz gauges, two scalar gluons couple to the quark, making all diagrams a factor $\frac{1}{v}$ stronger and hence contribute at the same order as the Abelian corrections in Fig. 8. Out of 25 scale-conserving diagrams, only eight survive the diagrammatic filter.

every vertex, the $Q^\dagger A_0 Q$ coupling is stronger in v than any other coupling, the NRQCD analogue to the non-Abelian QCD vertex correction to the scalar gluon vertex is sub-leading in the Feynman gauge. The resulting power counting is reported in Fig. 9. In the generalised Lorentz gauges, the scalar and vector components of the gauge field mix in the gluon propagation, with the amount of mixing proportional to $(1 - \alpha)$ (2.18). A scalar gluon emitted from a quark will therefore partially turn into a vector gluon, which then enters a three gluon vertex. The non-Abelian vertex corrections now have a non-trivial Lorentz structure and evaluate to be proportional to $(1 - \alpha)$ and $(1 - \alpha)^2$, as is confirmed

in App. A.2, (A.15). A factor $\frac{1}{v}$ is gained with respect to the power counting with one vector gluon coupling as given in Fig. 9, making the diagrams of the same, leading order as the Abelian vertex corrections. The non-Abelian graphs can consequently be seen as merely providing gauge corrections to the Abelian vertex result. The last diagram in the first row and the next-to-last in the second row of Fig. 9 are sub-leading and vanish using the equations of motion at lowest order for the outgoing potential quark, see App. A.2.

There is no comparable graph in QCD to the second category of non-Abelian vertex corrections in NRQCD at order g^3 . Figure 10 lists the topologies of all non-zero corrections to one gluon vertices involving one gluon loop. Again, one convinces oneself easily from

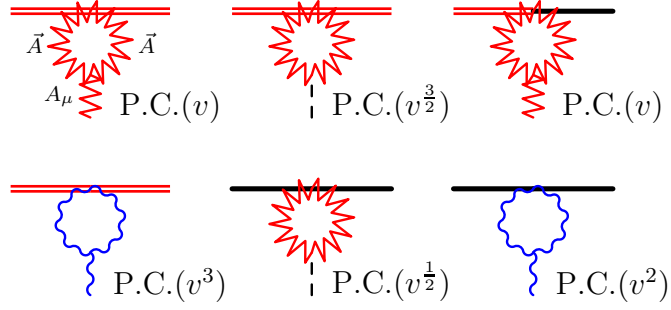


Figure 10: *The only non-zero diagrams of the vertex corrections of order g^3 from the Fermi term proportional to c_3 in the NRQCD Lagrangean (1.1). The soft blob in the next-to-last diagram provides an additional factor $\frac{1}{v}$ by loop power counting. The leading order power counting is obtained when the three gluon vertex is the standard QCD one and the gluons couple to the quark via the Fermi term. Out of 24 scale-conserving diagrams, only six survive the diagrammatic filter.*

tables 3 and 4 that these diagrams are at least one order in v weaker than the Abelian vertex corrections, even before the precise vertex structure is specified. In NRQED, this type of diagrams occurs first at order g^5 from the e_2 term in the Lagrangean (1.1) because a three photon coupling does not occur earlier. In QCD, the lowest order three gluon coupling is totally antisymmetric in colour space, so that its contraction with the totally symmetric expression in colour space from the vertex $\frac{g^2}{2M}Q^\dagger \vec{A}^2 Q$ vanishes. The Fermi interaction has a colour antisymmetric two gluon part because $B_i^a = \frac{1}{2}\epsilon^{ijk}(\partial_j A_k^a - \partial_k A_j^a + gf^{abc}A_j^b A_k^c)$, but is not a possible source of an order g^3 vertex correction in Fig. 10 to the minimal coupling of scalar gluons and quarks because the spin structures do not match.

Hence, the non-Abelian nature of the gauge field enters into the NRQCD β function only via the gluon vacuum polarisation and as what may be called gauge correction represented by non-Abelian vertex corrections. Each of the six quark gluon couplings between the various régimes is renormalised by one and only one non-zero Abelian and non-Abelian vertex correction.

Since the classification of diagrams following the rules of Sect. 3.2 is insensitive to the precise nature of the vertex coupling, the list leads as a by-product to a classification of

all non-zero one loop graphs in which two quarks and one gluon couple. The same is true for the quark self energy and vacuum polarisation graphs. The v power counting of the diagrams in Figs. 8, 9 and 10 is specific to the interactions chosen, but the fact that all other graphs with the same topology are zero is not.

All Abelian graphs lead to the same vertex vertex correction, as demonstrated in App. A.2 at exemplary graphs:

$$-i g_R \mu^\varepsilon t^a \Gamma^{\text{Abelian}}|_{\text{pole}} = \frac{i g_R^3 \mu^{3\varepsilon}}{8\pi^2} \left(C_F - \frac{N}{2} \right) t^a \frac{3-\alpha}{2} \Gamma[\varepsilon] \quad (3.28)$$

Likewise for the non-Abelian vertex corrections:

$$-i g_R \mu^\varepsilon t^a \Gamma^{\text{non-Abelian}}|_{\text{pole}} = \frac{-i g_R^3 \mu^{3\varepsilon}}{(4\pi)^2} \frac{N}{2} t^a \frac{3(1-\alpha)}{2} \Gamma[\varepsilon] \quad (3.29)$$

The vertex renormalisation in the $\overline{\text{MS}}$ scheme,

$$Z_1 = 1 - \Gamma^{\text{Abelian}}|_{\text{pole}} - \Gamma^{\text{non-Abelian}}|_{\text{pole}} , \quad (3.30)$$

coincides therefore with the one expected from the Slavnov–Taylor identities (3.27).

The NRQCD β function is computed from the scale invariance of the bare coupling

$$g = g_R \mu^\varepsilon \frac{Z_1}{Z_2 \sqrt{Z_3}} \quad (3.31)$$

and agrees with the anticipated result (3.1),

$$\beta_{\text{NRQCD}} = - \frac{g_R^3}{(4\pi)^2} \left[\frac{11}{3} N - \frac{2}{3} N_F \right] = \beta_{\text{QCD}} . \quad (3.32)$$

To the order calculated, one may “match” the relativistic and non-relativistic β functions to infer that indeed to lowest order in g and v ,

$$g_R^{\text{QCD}} = g_R^{\text{NRQCD}} . \quad (3.33)$$

To match NRQCD to QCD via the renormalisation group behaviour of its couplings and operators is of course considerably more complicated than to match matrix elements. Nonetheless, it demonstrates that matching relations survive renormalisation. The renormalised NRQCD coupling is as expected the same in all régimes, gauge invariant, and runs simultaneously in all régimes. The NRQCD β function is independent of the gauge parameter α . The Lorentz gauges are a legitimate gauge choice in NRQCD, obeying the Slavnov–Taylor identities. Wave function and vertex renormalisations differ in QCD and NRQCD, while the β functions do not.

In dimensionally regularised NRQCD, the vacuum polarisation receives its sole contribution from the propagation of on-shell relativistic particles, i.e. of physical soft or ultrasoft gluons and soft or ultrasoft ghosts and light quarks. Potential gluons, i.e. such mediating the Coulomb interaction, do not give rise to a gluon renormalisation, nor do

they contribute to *any* other renormalisation at lowest order in v , (3.19) and Figs. 6, 8 and 9. This observation applies to all standard gauges, including physical ones like the Coulomb gauge. It is traced back to the homogeneity of dimensional regularisation (3.10), which in turn is well known to be connected to a cancellation of ultraviolet and infrared divergences in scale-less integrals, e.g. [27, p. 172 f.]. In a cut-off regularisation, the situation is different as massless tadpoles require both infrared and ultraviolet regularisation resulting in logarithms, invalidating (3.10) and all diagrammatic rules, e.g. [28, Chap. 18.5]. In such a regularisation, the Coulomb gluon vacuum polarisation can therefore indeed receive its main contribution from Coulomb gluons in the intermediate state.

To close this section, mind that this derivation of the NRQCD β function is slightly simpler than its QCD counterpart but may be applied with equal generality. Except in the determination of the gluon vacuum polarisation, the Lorentz structure of the vertices and propagators did not enter. The Dirac algebra is not needed except when light fermions are included, and then the manipulations are straightforward. The vertex corrections in the Feynman gauge reduce to the computation of one graph: the Abelian vertex which involves neither Lorentz nor Dirac indices. Non-Abelian vertex corrections are easily extracted, see App. A.2. The presentation demonstrates also intuitively that quarks with mass M higher than the scale at which the β function is computed freeze out and are not to be included in the light quark number N_F of (3.32). In a world with N_f quarks, the QCD β function can hence be found from NRQCD with $N_f = N_F$ “light” quarks and one fictitious quark with a mass much bigger than any real quark mass.

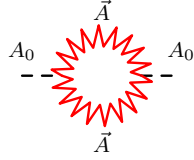
3.7 The Coulomb Gauge β Function

With the gauge independent classification of all one-loop self-energy, vacuum polarisation and vertex correction diagrams completed, it is straightforward to calculate the β function in the Coulomb gauge from the renormalisation of the scalar gluon field. In order to classify the contributing diagrams, one combines the notion that in the Coulomb gauge, A_0 is only potential (Sect. 2.2) with the knowledge of the topology of the non-zero one loop diagrams as reported in (3.19/3.21/3.22) and Figs. 8 to 10. As noted in the previous section, the leading order contribution in each self energy, vacuum polarisation or vertex correction graph is obtained when only scalar gluons couple to quarks, and when all gluons are on shell, i.e. either soft or ultrasoft. Because for the Coulomb gauge, this eliminates any correction which is of the same order as the quark propagator or the $Q^\dagger A_0 Q$ vertex (table 1), the soft and potential quark self energy and all vertex corrections, Abelian or non-Abelian, are therefore zero *to all orders* in g and v :

$$Z_1^{\text{Coulomb}} = 1 \quad , \quad Z_2^{\text{Coulomb}} = 1 \quad . \quad (3.34)$$

The coupling constant is hence renormalised only because the potential gluon vacuum polarisation in the Coulomb gauge is non-zero. A computation of the gluonic part which

makes again use of split dimensional regularisation can be found in [25, eq. (41)]:



$$: \Pi_{00}^{ab, \text{Coulomb}}(k) = \frac{i g_R^2 \mu^{2\varepsilon}}{(4\pi)^2} \delta^{ab} \vec{k}^2 \frac{11}{3} N \Gamma[\varepsilon] + \text{finite} \quad (3.35)$$

The ghost part is zero because ghosts do not propagate. The contribution for light fermions is gauge independent and can hence be extracted from the Lorentz gauge result (3.26). One arrives finally at

$$Z_3^{\text{Coulomb}} = 1 - \frac{g_R^2 \mu^{2\varepsilon}}{(4\pi)^2} \left[\frac{2}{3} N_F - \frac{11}{3} N \right] \Gamma[\varepsilon] . \quad (3.36)$$

Not surprisingly, the NRQCD β function is extracted as (3.32) using (3.31). This particular part of renormalising NRQCD in the Coulomb gauge may appear simpler than in the Lorentz gauges, but other parts suffer severely from technical problems like the non-transversality of the gluon propagator.

4 Conclusions and Outlook

After presenting the extension to NRQCD of a recently proposed explicit velocity power counting scheme for a non-relativistic toy field theory [15] following Beneke and Smirnov's threshold expansion [16], this article presented the computation of the NRQCD β function to lowest order in g and v in the Lorentz gauges and in the Coulomb gauge. It endorsed the relevance of a new quark representative and a new gluon representative in the soft scaling régime $E \sim |\vec{p}| \sim Mv$ in which quarks are static and gluons on shell. HQET becomes a sub-set of NRQCD. The identification of three different régimes of scale for on-shell particles from the poles of the NRQCD propagators leads in a natural way to this régime, in addition to the well known potential one with on-shell quarks and instantaneous gluons mediating the Coulomb binding [14] and the ultrasoft one with bremsstrahlung gluons [19]. Neither of the five fields in the three régimes should be thought of as “physical particles”. Rather, they represent the “true” quark and gluon in the respective régimes as the infrared-relevant degrees of freedom. None of the régimes overlap. Using a rescaling technique [14, 18, 19], Sect. 2 proposed an NRQCD Lagrangean which leads to the correct behaviour of scattering and production amplitudes [15]. It establishes explicit velocity power counting, preserved to all orders in perturbation theory once dimensional regularisation is chosen to complete the theory. The reason is the non-commutativity of the expansion in small parameters with dimensionally regularised integrals and the homogeneity of dimensional regularisation.

There is an intimate relation between the recently discovered threshold expansion [16] and this version of NRQCD which uses dimensional regularisation and has been developed over the past years [14, 15, 18, 19]. This was demonstrated at the outset of the computation of the β function in Sect. 3.1 and has already led to fruitful exchange. As noted by Beneke and Smirnov [16], threshold expansion provides an efficient way to derive the

NRQCD Lagrangean (1.1) from QCD, deepening our understanding of effective field theories: The coefficients c_i, d_i, e_i are obtained by computing QCD diagrams and sub-diagrams in the hard régime, $q \sim M$. Threshold expansion also shows how to systematise identifying the different kinematic régimes of NRQCD. Indeed, NRQCD was incomplete without the soft régime and its corresponding degrees of freedom as pointed out by Beneke and Smirnov [16]. One might therefore see threshold expansion and NRQCD as two sides of the same coin. The one expands loop integrals to establish a power counting for Feynman diagrams, while the other uses rescaling properties to classify the relative strengths of all vertices, allowing for intuitive interpretations of the derived vertex power counting rules on the level of the Lagrangean (see the end of Sect. 2.3). An effective field theory formulation can also be applied more easily to bound state problems. Finally, while threshold expansion has not yet been proven to be valid on a formal level, the existence of NRQCD as an effective field theory is guaranteed by the renormalisation group, e.g. [26, Chap. 8].

The calculation of the NRQCD β function in the Lorentz gauges to one loop order in Sect. 3 – albeit its result was easily anticipated – was non-trivial as it demonstrated that the power counting proposed is consistent also after renormalisation. Because of the splitting of quark and gluon fields in different representatives in the various régimes, this might be thought not to be straightforward. It also resolved a puzzle about the running of the coupling of gluons mediating the Coulomb interaction. The rescaling and power counting rules are gauge independent for a wide class of gauges including all standard gauges. Bare graphs and their corrections are of the same power in v . The soft régime is necessary not only to render the same β function as in QCD, but even to attain a result which is independent of the gauge parameter α at all and in which the renormalisation constants obey the Slavnov–Taylor identities. In the Coulomb gauge calculation of the β function, the quark self energy and the vertex correction of the vertex coupling a quark minimally to a scalar gluon is easily shown to be zero to all orders in g and v . In the Coulomb gauge, the vacuum polarisation is therefore the only non-trivial renormalisation necessary for the β function.

The derivation was greatly simplified by diagrammatic rules (Sect. 3.2) which follow from the homogeneity property of dimensional regularisation and allow one to systematically recognise the majority of NRQCD graphs as zero to all orders in v just by drawing them, independently of the gauge and of details of the vertices involved. The rules apply equally well to threshold expansion and will prove fruitful in more rigorous investigations, also into NRQCD. Here, they were already used to prove scale conservation and the decoupling of the ultrasoft, heavy quark in Sect. 3.3. All topologies of one loop corrections to vertices involving one gluon and one quark were also classified, and the power counting of the leading order contributions determined.

Dimensional regularisation in NRQCD has many advantages over other regularisation schemes in which scale-less integrals are non-zero. It preserves the symmetries and guarantees the tree level power counting to be corrected at most by logarithms. It is well known that cut-off regularisation violates gauge symmetry and wants removal of power divergences in the renormalisation process in order to conserve the tree level power counting to all orders. When massless tadpoles do not vanish, the number of diagrams to be

computed in order to obtain even a simple vertex correction was seen to increase from one in dimensional regularisation to three or more. In general, it is not clear whether scale conservation holds in cut-off regularisation: The three different régimes require the introduction of at least three artificial cut-off scales to separate them and to cure ultra-violet divergences. Furthermore, the ultrasoft quark does not decouple, adding further diagrams. In the end, the answers of all well-defined regularisation schemes do agree, but dimensional regularisation provides an elegant way which furthermore often leads to analytic expressions. A disadvantage of dimensional regularisation is that in its standard formulation, it cannot be used to explore the non-perturbative sector of NRQCD.

Finally, NRQCD with dimensional regularisation shows how to establish a power counting in any effective field theory with several low energy scales: The theory is first divided into one sector containing the particles relativistic at a given heavy scale and another sector containing the non-relativistic particles. In NRQCD, the former are light quarks, gluons and ghosts, the latter the heavy quark. The effect of all physics at larger scales is absorbed into the coefficients of the Lagrangean. Then, one identifies the combinations of scales in which particles become on shell by looking at the denominators of the various propagators. This gives the scaling régimes. Finally, the Lagrangean is rescaled to dimensionless fields in each régime to exhibit the vertex and loop power counting rules. A priori, all couplings obeying scale conservation are allowed. The diagrammatic rules developed in Sect. 3.2 still hold. Non-relativistic effective nuclear field theory is one obvious application with three low energy scales: the pion mass and production threshold, and the anomalously large scattering length of the two body system ⁴.

Among the points to be addressed further is an extension of the diagrammatic rules. An investigation of the influence of soft quarks and gluons on bound state calculations in NRQED and NRQCD is also important because – as seen at the end of Sect. 2.4 – their contribution at $\mathcal{O}(g^4)$ and higher becomes stronger than retardation effects. To investigate the non-perturbative sector of NRQCD and to establish its equivalence to QCD in the continuum is another formidable task.

Acknowledgements

I am indebted to M. Luke for initial discussions about the problem of the β function in power counted NRQCD out of which this article grew, and to M. Burkardt, J. Gasser, G. P. Lepage, H. Reinhardt, A. Pineda, M. J. Savage and J. Soto for valuable further exchanges and discussions. The work was supported in part by a Department of Energy grant DE-FG03-97ER41014.

⁴Following this article, Mehen and Stewart investigated the soft régime in effective nuclear theory [29].

A Some Details on Split Dimensional Regularisation

A.1 Useful Split Dimensionally Regularised Integrals

This appendix presents some useful formulae for non-covariant loop integrals using split dimensional regularisation as introduced by Leibbrandt and Williams [25], see also the Appendix in [15]. In its results, split dimensional regularisation agrees with other methods to compute loop integrals in non-covariant gauges, such as the non-principal value prescription [30], but two features make it especially attractive: It treats the temporal and spatial components of the loop integrations on an equal footing, and no recipes are necessary to deal with e.g. pinch singularities. Rather, it uses the fact that, like in ordinary integration, the axioms of dimensional regularisation [26, Chap. 4.1] allow to split the integration into two separate integrals:

$$\int \frac{d^d k}{(2\pi)^d} = \int \frac{d^\sigma k_0}{(2\pi)^\sigma} \frac{d^{d-\sigma} \vec{k}}{(2\pi)^{d-\sigma}} \quad (\text{A.1})$$

Where applicable, split and ordinary dimensional regularisation of covariant integrals must hence agree once the limit $\sigma \rightarrow 1$ is taken with d still arbitrary.

For the quark self energy, the integral

$$\int \frac{d^d q}{(2\pi)^d} \frac{1}{(q^2 + i\epsilon)^\alpha} \frac{1}{q_0 + a + i\epsilon} \quad (\text{A.2})$$

is most easily computed by combining denominators as in HQET,

$$2\alpha \int_0^\infty d\lambda \int \frac{d^d q}{(2\pi)^d} [q^2 + 2\lambda(q_0 + a) + i\epsilon]^{-(\alpha+1)} . \quad (\text{A.3})$$

Now, the integrand is in a standard covariant form and can be computed using Minkowski space methods with the result

$$\int \frac{d^d q}{(2\pi)^d} \frac{1}{(q^2 + i\epsilon)^\alpha} \frac{1}{q_0 + a + i\epsilon} = \frac{2i \Gamma[\frac{d}{2} - \alpha] \Gamma[2\alpha + 1 - d]}{(4\pi)^{\frac{d}{2}} \Gamma[\alpha]} (2a + i\epsilon)^{d-(2\alpha+1)} e^{i\pi(\frac{d}{2}-\alpha)} . \quad (\text{A.4})$$

By differentiating with respect to a , the following formula useful for the computation of the vertex corrections is derived:

$$\int \frac{d^d q}{(2\pi)^d} \frac{1}{(q^2 + i\epsilon)^\alpha} \frac{1}{(q_0 + a + i\epsilon)^\beta} = \frac{2i \Gamma[\frac{d}{2} - \alpha] \Gamma[2\alpha + \beta - d]}{(4\pi)^{\frac{d}{2}} \Gamma[\alpha] \Gamma[\beta]} (2a + i\epsilon)^{d-2\alpha-\beta} e^{i\pi(\frac{d}{2}-\alpha)} \quad (\text{A.5})$$

Another generalisation is easiest computed by first combining the denominators linear in q_0 using Feynman parameters,

$$\frac{1}{q_0 + a + i\epsilon} \frac{1}{q_0 + b + i\epsilon} = \int_0^1 dx \frac{1}{[q_0 + xa + (1-x)b + i\epsilon]^2} , \quad (\text{A.6})$$

and employing (A.5):

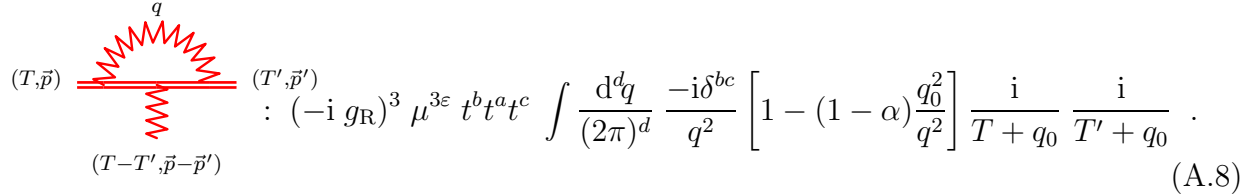
$$\begin{aligned} \int \frac{d^d q}{(2\pi)^d} \frac{1}{(q^2 + i\epsilon)^\alpha} \frac{1}{q_0 + a + i\epsilon} \frac{1}{q_0 + b + i\epsilon} = \\ = \frac{-2i \Gamma[\frac{d}{2} - \alpha] \Gamma[2\alpha + 1 - d]}{(4\pi)^{\frac{d}{2}} \Gamma[\alpha]} \frac{(2a + i\epsilon)^{d-2\alpha-1} - (2b + i\epsilon)^{d-2\alpha-1}}{a - b} e^{i\pi(\frac{d}{2} - \alpha)} \end{aligned} \quad (\text{A.7})$$

Note that in all three integrals (A.4/A.5/A.7), a shift of \vec{q} by an arbitrary value leaves the result unaffected. A scale in the momentum integration is only induced by the scales a, b of the energy integration.

A.2 Computation of Exemplary Vertex Corrections

In order to illustrate the NRQCD power counting scheme further, this appendix outlines the computation of characteristic Abelian and non-Abelian vertex corrections in Sect. 3.6.

The Feynman rules give for the Abelian correction to the $Q_s^\dagger A_{s,0} Q_s$



$$: (-i g_R)^3 \mu^{3\epsilon} t^b t^a t^c \int \frac{d^d q}{(2\pi)^d} \frac{-i\delta^{bc}}{q^2} \left[1 - (1-\alpha) \frac{q_0^2}{q^2} \right] \frac{i}{T+q_0} \frac{i}{T'+q_0} . \quad (\text{A.8})$$

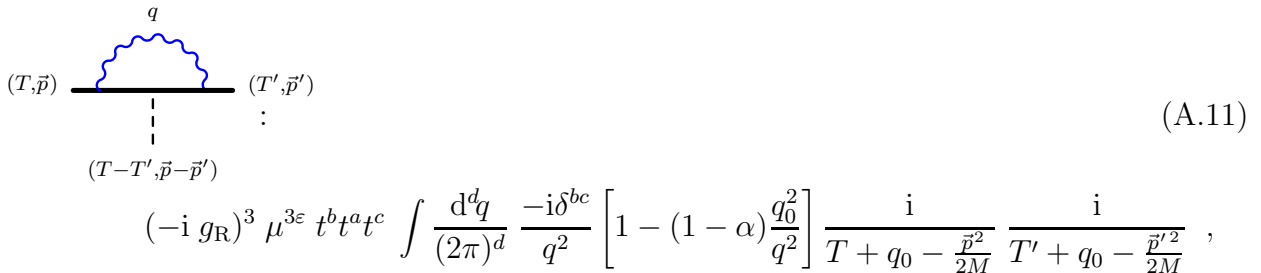
As usual, $t^b t^a t^b = (C_F - \frac{N}{2}) t^a$. The integral containing q_0^2 in the numerator is simplified by re-writing it as

$$\frac{q_0^2}{(T+q_0)(T'+q_0)} = 1 + \frac{TT'}{(T+q_0)(T'+q_0)} - \frac{T}{(T+q_0)} - \frac{T'}{(T'+q_0)} \quad (\text{A.9})$$

and noting that the first integral is zero as it is without scale (3.10). The remaining integrals are using (A.4/A.7)

$$\frac{i g_R^3 \mu^{3\epsilon}}{8\pi^2} \left(C_F - \frac{N}{2} \right) t^a \frac{3-\alpha}{2} \Gamma[\epsilon] + \text{finite}, \quad (\text{A.10})$$

from which (3.28) is read up. The Abelian correction to $Q_p^\dagger A_{p,0} Q_p$,



$$: (-i g_R)^3 \mu^{3\epsilon} t^b t^a t^c \int \frac{d^d q}{(2\pi)^d} \frac{-i\delta^{bc}}{q^2} \left[1 - (1-\alpha) \frac{q_0^2}{q^2} \right] \frac{i}{T+q_0 - \frac{\vec{p}^2}{2M}} \frac{i}{T'+q_0 - \frac{\vec{p}'^2}{2M}} , \quad (\text{A.11})$$

is inferred by replacing $T \rightarrow T - \frac{\vec{p}^2}{2M}$ and $T' \rightarrow T' - \frac{\vec{p}'^2}{2M}$ in (A.10). Again, Γ^{Abelian} is extracted as quoted in (3.28). Note that – if one were to employ the equations of motion

for the outgoing particles – the integral would appear to vanish as no scale is present. This would mean that there is no Abelian vertex correction to the potential (or ultrasoft) scalar gluon vertex. In that case, the result for the NRQCD β function is not even gauge invariant. Since the diagram is the leading order contribution to the correction of the $Q_p^\dagger A_{p,0} Q_p$ vertex (Fig. 8), the application of the equations of motion is not legitimate.

As noted in Sect. 3.6, there are two Abelian corrections to $Q_s^\dagger A_{s,0} Q_p$. The leading one is

$$(T, \vec{p}) \text{ --- } (T', \vec{p}') : (-i g_R)^3 \mu^{3\varepsilon} t^b t^a t^c \int \frac{d^d q}{(2\pi)^d} \frac{-i\delta^{bc}}{q^2} \left[1 - (1 - \alpha) \frac{q_0^2}{q^2} \right] \frac{i}{q_0} \frac{i}{T + q_0} . \quad (\text{A.12})$$

(T-T' → T, $\vec{p}-\vec{p}'$)

The integration (A.4/A.7) gives the expected Abelian contribution (3.28) to the vertex normalisation (3.27).

The vertex correction already discussed in connection with the cutting rule, (3.13), is according to Sec. 3.6 of order v^1 and hence not the leading contribution. Because $T' \sim \frac{\vec{p}'^2}{2M} \sim Mv^2$ and $T \sim |\vec{p}| \sim Mv$, one indeed finds

$$(T, \vec{p}) \text{ --- } (T', \vec{p}') : (-i g_R)^3 \mu^{3\varepsilon} t^b t^a t^c \int \frac{d^d q}{(2\pi)^d} \frac{-i\delta^{bc}}{q^2} \left[1 - (1 - \alpha) \frac{q_0^2}{q^2} \right] \frac{i}{T} \frac{i}{T' + q_0 - \frac{\vec{p}'^2}{2M}} =$$

$$(T, \vec{p} - \vec{p}') = \frac{i g_R^3 \mu^{3\varepsilon}}{8\pi^2} \left(C_F - \frac{N}{2} \right) t^a \frac{3 - \alpha}{2} \Gamma[\varepsilon] \frac{T' - \frac{\vec{p}'^2}{2M}}{T} + \text{finite} = \text{P.C.}(v)! \quad (\text{A.13})$$

The diagram will therefore only contribute to the renormalisation of the multipole expansion. Moreover, because it is sub-leading, one may use inside the integral the equations of motion at leading order in the power counting, $T = \frac{\vec{p}^2}{2M}$, to set the outgoing potential quark on its mass-shell. The integral vanishes then, as no scale is present, see (3.13) and (A.13).

The cutting rule suggests that the $Q_s^\dagger A_{u,0} Q_s$ correction should be related to the soft quark self energy:

$$(T, \vec{p}) \text{ --- } (T', \vec{p}') \xrightarrow{(T-T' \rightarrow 0, \vec{p}-\vec{p}' \rightarrow 0)} : (-i g_R)^3 \mu^{3\varepsilon} t^b t^a t^c \int \frac{d^d q}{(2\pi)^d} \frac{-i\delta^{bc}}{q^2} \left[1 - (1 - \alpha) \frac{q_0^2}{q^2} \right] \frac{i}{T + q_0} \frac{i}{T + q_0} \quad (\text{A.14})$$

The dot at the cut-off vertex stands again as a reminder that the structure of the vertex will enter here, and one finds the vertex correction to be proportional to $\frac{\partial}{\partial T} \Sigma_s(T, \vec{p})$ (3.21). Using (A.5), the vertex correction is again (3.28).

Finally, two examples for the straightforward but tedious non-Abelian vertex corrections of Fig. 9 are given. First, one may calculate the non-Abelian correction to $Q_s^\dagger A_{u,0} Q_s$

$$: (-i g_R)^2 g_R \mu^{3\varepsilon} f^{abc} t^b t^c \int \frac{d^d q}{(2\pi)^d} \frac{i}{T+q_0} \frac{i\mathcal{G}^{0\mu}(q)}{q^2} \frac{i\mathcal{G}^{0\nu}(q)}{q^2} \times$$

$$\times [-2q_0 g_{\mu\nu} + q_\mu g_{\nu 0} + q_\nu g_{\mu 0}] \quad . \quad (\text{A.15})$$

The Feynman gauge term, being independent of $(1-\alpha)$, is zero as expected. For this diagram, even the terms proportional to $(1-\alpha)^2$ vanish, which can be shown to be finite in general and hence not to contribute to the vertex normalisation. In (A.15), only the contribution leading in v is considered. Using the well known relation $if^{abc}t^a t^b = -\frac{N}{2}t^a$ for $SU(N)$, this can be collapsed down by re-writing numerators analogously to (A.9) to

$$g_R^3 \mu^{3\varepsilon} N t^a (1-\alpha) T \int \frac{d^d q}{(2\pi)^d} \frac{1}{T+q_0} \frac{1}{q^4} \left[\frac{T^2}{q^2} - 1 \right] \quad . \quad (\text{A.16})$$

One extracts the pole part of the non-Abelian vertex correction as (3.29) from the result obtained using (A.4):

$$\frac{-i g_R^3 \mu^{3\varepsilon}}{(4\pi)^2} \frac{N}{2} t^a \frac{3(1-\alpha)}{2} \Gamma[\varepsilon] + \text{finite}. \quad (\text{A.17})$$

The leading piece of the non-Abelian correction to $Q_p^\dagger A_{p,0} Q_p$ is extracted as

$$: (-i g_R)^2 g_R \mu^{3\varepsilon} f^{abc} t^b t^c \int \frac{d^d q}{(2\pi)^d} \frac{i}{q_0} \frac{i\mathcal{G}^{0\mu}(q)}{q^2} \frac{i\mathcal{G}^{0\nu}(q+\Delta E)}{(q+\Delta E)^2} \times$$

$$\times [2q_0 g_{\mu\nu} + (\Delta E - q)_\mu g_{\nu 0} - (q + 2\Delta E)_\nu g_{\mu 0}] \quad , \quad (\text{A.18})$$

where $\Delta E = (0, \vec{p}' - \vec{p})$. The term proportional to $(1-\alpha)$ contains the ultraviolet singularity and can be written as

$$- g_R^3 \mu^{3\varepsilon} N t^a (1-\alpha) \int \frac{d^d q}{(2\pi)^d} \frac{1}{q^4} \frac{1}{(q+\Delta E)^2} (q_0^2 - q^2 - 2E \cdot q) \quad . \quad (\text{A.19})$$

Standard formulae for dimensional regularisation yield as divergent part (3.29). The term proportional to $(1-\alpha)^2$ is ultraviolet finite and can be reduced to the integral

$$g_R^3 \mu^{3\varepsilon} \frac{N}{2} t^a (1-\alpha)^2 \Delta E^2 \int \frac{d^d q}{(2\pi)^d} \frac{q_0^2}{q^4} \frac{1}{(q+\Delta E)^4} = \frac{i g_R^3 \mu^{3\varepsilon}}{(4\pi)^2} \frac{N}{2} t^a \frac{(1-\alpha)^2}{2} \quad . \quad (\text{A.20})$$

References

- [1] W. E. Caswell and G. P. Lepage: *Phys. Lett. B* **167**, 437 (1986).
- [2] G. T. Bodwin, E. Braaten and G. P. Lepage: *Phys. Rev. D* **51**, 1125 (1995); *Phys. Rev. D* **55**, 5853 (1997).
- [3] M. Nio and T. Kinoshita: *Phys. Rev. D* **55**, 7267 (1997).
- [4] A. H. Hoang, P. Labelle and S. M. Zebarjad: *Phys. Rev. Lett.* **79**, 3387 (1997).
- [5] A. H. Hoang and T. Teubner: *Top Quark Pair Production at Threshold: Complete Next-to-next-to-leading Order Relativistic Corrections*; hep-ph/9801397, 1998 (to be published).
- [6] A. Pineda and J. Soto: *Potential NRQED: The Positronium Case*; UB-ECM-PF 98/11, KFA-IKP(TH)-98-9, hep-ph/9805424, 1998 (to be published).
- [7] C. T. H. Davies for the NRQCD Collaboration: *Nucl. Phys. (Proc. Suppl.)* **63**, 320 (1998).
- [8] H. Matsufuru et al.: *Nucl. Phys. (Proc. Suppl.)* **63**, 368 (1998).
- [9] A. Czarnecki and K. Melnikov: *Phys. Rev. Lett.* **80**, 2531 (1998).
- [10] M. Jezabek et al.: *Phys. Rev. D* **58**, 14006 (1998).
- [11] E. Braaten: *Introduction to the NRQCD Factorization Approach to Heavy Quarkonium*; hep-ph/9702225, 1997 (talk given at the third International Workshop on Particle Physics Phenomenology, Taipei, Taiwan, 14–17 Nov 1996).
- [12] N. Brambilla and A. Vairo: *Some Aspects of the Quark-Antiquark Wilson Loop Formalism in the NRQCD Framework*; hep-ph/9809230, 1998 (to be published in the Proceedings of the Euroconference QCD'98 at Montpellier, 2nd – 8th July 1998, *Nucl. Phys. B*(Proc. Suppl.)).
- [13] A. V. Manohar: *Phys. Rev. D* **56**, 230 (1997).
- [14] M. Luke and A. V. Manohar: *Phys. Rev. D* **55**, 4129 (1997).
- [15] H. W. Griesshammer: *Phys. Rev. D* **58**, 094027 (1998).
- [16] M. Beneke and V. A. Smirnov: *Nucl. Phys. B* **522**, 321 (1998).
- [17] C. Bauer and A. V. Manohar: *Phys. Rev. D* **57**, 337 (1998).
- [18] M. Luke and M. J. Savage: *Phys. Rev. D* **57**, 413 (1998).
- [19] B. Grinstein and I. Z. Rothstein: *Phys. Rev. D* **57**, 78 (1998).

- [20] H. W. Griebhammer: *The Soft Régime in NRQCD*; NT@UW-98-12, hep-ph/9804251, 1998 (Proceedings of the Workshop “Nuclear Physics With Effective Field Theories” at Caltech, 26th – 27th February 1998, eds. R. Seki, U. van Kolck and M. J. Savage, World Scientific, p. 229).
- [21] G. P. Lepage et al.: *Phys. Rev. D* **46**, 4052 (1992).
- [22] P. Labelle: *Phys. Rev. D* **58**, 093013 (1998).
- [23] N. Isgur and M. B. Wise: *Phys. Lett. B* **232**, 113 (1989).
- [24] N. Isgur and M. B. Wise: *Phys. Lett. B* **237**, 527 (1990).
- [25] G. Leibbrandt and J. Williams: *Nucl. Phys. B* **475**, 469 (1996).
- [26] J. Collins: *Renormalization*; Cambridge Monographs on Mathematical Physics, CUP (1984).
- [27] T. Muta: *Foundations of Quantum Chromodynamics*; Lecture Notes in Physics Vol. 5, World Scientific (1987).
- [28] T. D. Lee: *Particle Physics and Introduction to Field Theory*; revised and updated first edition, Contemporary Concepts in Physics Vol. 1, Harwood Academic Publishers (1988).
- [29] T. Mehen and I. W. Stewart: *Radiation Pions in Two-Nucleon Effective Field Theory*; CALT-68-2210, nucl-th/9901064, 1999 (to be published).
- [30] K.-C. Lee and S.-L. Nyeo: *J. Math. Phys.* **35**, 2210 (1994).
- [31] P. Ramond: *Field Theory: A Modern Primer*; Frontiers in Physics Vol. 74, Addison Wesley (1990).